MECHANICAL AND MATERIAL PROPERTIES OF AIR ENTRAINED HIGH STREGTH CONCRETE AT ELEVATED TEMPERATURES

By

Farhan Waheed

(NUST201362257MSCEE15213F)

Master of Science

In

Structural Engineering

NUST Institute of Civil Engineering (NICE)

School of Civil and Environmental Engineering (SCEE)

National University of Sciences and Technology (NUST) Islamabad, Pakistan

This is to certify that the

thesis titled

MECHANICAL AND MATERIAL PROPERTIES OF AIR ENTRAINED HIGH STREGTH CONCRETE AT ELEVATED TEMPERATURES

submitted by

Farhan Waheed

NUST201362257MSCEE15213F

has been accepted towards the partial fulfillment

of the requirements for the degree

of

Master of Science

in

Structural Engineering

_____

Dr. Rao Arsalan Khushnood (Advisor)

Assistant Professor

NUST Institute of Civil Engineering (NICE)

School of Civil and Environmental Engineering (SCEE)

National University of Sciences and Technology (NUST), Islamabad, Pakistan

THESIS ACCEPTANCE CERTIFICATE

Certified that final copy of MS/MPhill thesis written by Mr Farhan Waheed Registration No. NUST201362257MSCEE15213F of MS Structural Engg Fall 2013 Batch (NICE) has been vetted by under-signed, found completed in all respects as per NUST Statutes/Regulations, is free of plagiarism, errors, and mistakes and is accepted as partial fulfillment for award of MS/MPhil degree. It is further certified that necessary amendments as pointed out by GEC members of the scholar have been incorporated in the said thesis

Signature _____

Name of Supervisor Dr. Rao Arsalan Khushnood

Date:_____

Signature (HoD) _____

Date:_____

Signature (Dean/Principal)_____

Date:_____

DEDICATED

TO

MY GRAND PARENTS

ACKNOWLEDGEMENTS

ABSTRACT

The performance of high strength concrete (HSC) under fire conditions is an established concern in concrete industry. The kinetics and mechanisms involved in processes that affect the fire behavior of HSC are mostly controlled by its mechanical and material properties, thermo-mechanical interactions, and type of structural component exposed to fire. The weaknesses of HSC in infrastructure under fire conditions preclude its applications in fire resistance applications unless significant modifications are done either to concrete mix or the structural design. For many years, polypropylene fibers have been used to attain a certain amount of essential porosity in HSC under fire resistance applications. Air entrained HSC however, can provide a suitable alternative to conventional HSC under fire conditions, especially due to its permeability properties in hardened state. An experimental program was designed to obtain high strength air entrained concrete and study its performance at elevated temperatures in 23 to 800°C temperature range. In this study, material properties of air entrained HSC at varying air volume of 4% and 8% were investigated and compared with conventional HSC at elevated temperatures for residual and unstressed test conditions. Mechanical tests namely compressive strength, splitting tensile strength, stress-strain response, elastic modulus, and spalling behavior under a relatively higher heating rate of 10°C/min were studied. Additionally, changes in physical properties consisting of mass loss, scattered electron microscopy analysis and cracking behavior were also carried out. Results show that air entrained concrete performed better at elevated temperature with improved mechanical properties and spalling mitigation. Conversely, an increased air content in concrete did not depict a performance improvement at elevated temperatures.

TABLE OF CONTENTS

LIST OF FIGURES

x

LIST OF TABLES

CHAPTER 1

INTRODUCTION

1.1   General

Concrete is such an old material that it has been known from years. Historical structures built up using concrete as a main structural material can be found these days like pantheon's dome which was constructed 2000 years ago in Rome, Italy (Lamprecht 1993). Concrete possess a key place among others in materials of civil engineering due to its strength, durability, ease in manufacturing, and fire endurance. Concrete being a main load bearing construction material is always used and designed to withstand primary loads on structures. In addition to the primary loads there exist some environmental threats such as earth quake, blast, flood, and fire etc. Under these prescribed environmental threats fire incident is the only one which effects directly on the concrete material and causes physical and microstructural changes in it. Therefore, the knowledge of effect of fire on material changes in concrete is necessary in order to design concrete structures capable to withstand fire incident. Concrete is quite safe when the structure is exposed to routine temperature, but there exist some serious threats of fire incident in a structure which can cause deleterious effects on concrete.

Fire has very destructive effects on the vital properties of concrete. Decrease in mechanical properties especially in compressive strength, decrease in elastic modulus and increase in permeability, porosity and increased chances of spalling all are outcomes of elevated temperature which is caused by a fire incident. High Strength Concrete (HSC) has its own peculiar behavior under elevated temperature which is very much different from Normal Strength Concrete (NSC).

The knowledge and usage of water reducers, high range water reducing agent and pozzolans (natural or artificial) or Secondary Raw Materials (SRMs) coined the concrete type HSC, which is now widely being used in construction industry. By the virtue of its very high strength larger dimensional cross sections of concrete structures are shrunk into smaller dimension cross sections especially the concrete columns. HSC is a very big advancement in concrete industry and is being used vastly in concrete structures, but fire damage to HSC is more severe than NSC. Although several techniques are available through which fire behavior of HSC can be improved, addition of polypropylene (PP) fibers is most common among them, but still the topic of improvement in fire behavior of HSC needs to be addressed. Entraining air in HSC is envisaged to be a quite good technique and its efficiency is studied in this research program.

1.2   Air entrained concrete

The free moisture content in concrete can never be avoided, although minimum w/c ratio to complete the hydration process of cement is 0.24, but this is not practical. Expansion and contraction of water due to freeze thaw cycles induces internal stresses in concrete which is the reason of scaling of concrete especially in rigid pavements. Scaling is defined by the Portland Cement Association (PCA) as "a general loss of surface mortar or mortar surrounding the coarse aggregate particles on a concrete surface. This problem is typically caused by the expansion of water due to freezing and thawing cycles and the use of deicing chemicals" So, to resist the deterioration caused by this freeze thaw phenomenon small air bubbles in concrete in its fresh state during mixing are intentionally introduced which are well spread along the volume of concrete and remain there in hardened state as well. Now, these tiny air bubbles provide space to the water to expand without inducing internal stresses in concrete thus scaling is avoided. Now Air Entrained

Concrete (AEC) can be defined "The conventional concrete in which tiny air bubbles are intentionally introduced mainly to resist against deterioration caused by freezing and thawing of water in concrete or to increase the workability of low cement concrete is known as AEC."

AEC was developed in quite inadvertent way. Jackson (1944) reported that blend of Ordinary Portland Cement (OPC) and natural cement containing tallow or crusher oil is more durable against surface scaling caused due to de-icing of pavements, when de-iced with the help of salts or cinders. The air entrained in concrete due to above described composition was the primary reason of improvement in durability. It opened a new gateway in the concrete world and AEC came up with a new area of concrete used extensively to fight against the destruction caused by freezing and thawing of concrete.

Jackson and Timms (1954) studied 27 different materials and evaluated their air entrainment capabilities along with effect on flexure and compressive strength of concrete. These materials are categorized as Salts of Wood Resins, Synthetic Detergents, Salts of Sulfonated Lignin, Salts of Petroleum acids, Salts of proteinaceous materials, Fatty and resinous acids and their salts and Organic salts of sulfonated hydrocarbons. Generally, air quantity equal to 5% to 6% of total volume of fresh concrete is adequate to make concrete durable against scaling or mass loss under freeze thaw cycles. It is observed that concrete specimens having entrapped air of 2% and 2.3% lose their mass by 25% on just 100 and 190 cycles respectively. Whereas specimens having entrained air ranging from 5.5% to 6.5% can bear 200 cycles with a non-considerable mass loss (Jackson 1944; Shang and Yi 2013), which clearly describes the importance of entrainment of air when freeze-thaw durability is in question. There is no experimental data available on AEC at elevated temperature. The understandings based on the previous knowledge of testing of concrete

15

with PP fibers say that AEC will give a better response under fire. So, it is expected that AEC will improve the fire behavior in terms of both i.e. loss in mechanical strength and spalling.

1.3   High strength concrete

As the name indicates, HSC means the concrete with higher compressive strength than normal or conventional concrete. The primary discrimination between HSC and NSC is the difference in their 28-days compressive strength. The threshold strength value which discriminates between HSC and NSC is not clear among standards and authors. This threshold value keeps on varying among different journals and standards. ACI 211.4-08 (2008) defines concrete having compressive strength greater than 41.25 MPa (6000 psi) as HSC. The threshold value of strength given by ACI 211.4-08 (2008) in this study is considered as lowest strength of HSC.

There are two different chemical compositions which are used to increase the strength of conventional concrete to make it HSC. These are water reducers or high range water reducers and SRMs. Decreasing the w/c of concrete increases its compressive strength but on the other hand workability of concrete which is defined as "ease with which the concrete can be handled, mixed or placed" (ACI 2013) is also lost. Owing to this loss, concrete placement and consolidation is nearly impossible which results in large voids of entrapped air causing decrease in its strength in hardened state. HRWRs are added during the mixing stage of concrete and these are very effective to achieve the workability at very less w/c ratio.

Other chemical composition besides chemical admixtures are mineral admixtures (natural or artificial) which are also known as SRMs or supplementary cementitious materials or simply pozzolans. ACI 211.4-08 (2008) defines them as "a siliceous or siliceous and aluminous material that in itself possesses little or no cementitious value but that will, in finely divided form and in

the presence of moisture, chemically react with calcium hydroxide at ordinary temperatures to form compounds having cementitious properties". Using these two chemical compositions namely water reducers and supplementary raw materials, the mechanical strength of concrete can be increased with much effectiveness.

1.3.2   Fire Behavior of High Strength Concrete

Performance of NSC under fire is excellent and this fact is widely accepted by all of the researchers. Fire performance of NSC shows less drop in strength (compressive and tensile), low mass loss, less drop in stress-strain modulus and less chances of spalling. Owing to this behavior concrete is used in so many structures exposed to fire. Concrete structures, when fire incident happens, give sufficient and adequate time not only to the occupants for evacuating but also to fire fighters for mitigation of fire. But all this is true for normal strength concrete having pores in hardened state due to increased water content.

Converse to the NSC, HSC has rapid strength loss, higher drop in modulus and frequent spalling as shown in the following Fig 1.1. Another very destructive effect of fire which is more pronounced in HSC specially in concrete which contains Silica Fume, is spalling of concrete cover as observed by Sanjayan et al. (1993) . The improved microstructure of HSC results decrease in porosity. The lesser porosity in HSC is the reason of explosive spalling phenomenon is HSC. This explanation is validated by the tests performed by Zeiml et al. (2006). The addition of PP fibers increases the concrete permeability at temperature higher than melting point of fibers used which renders spalling less frequent.
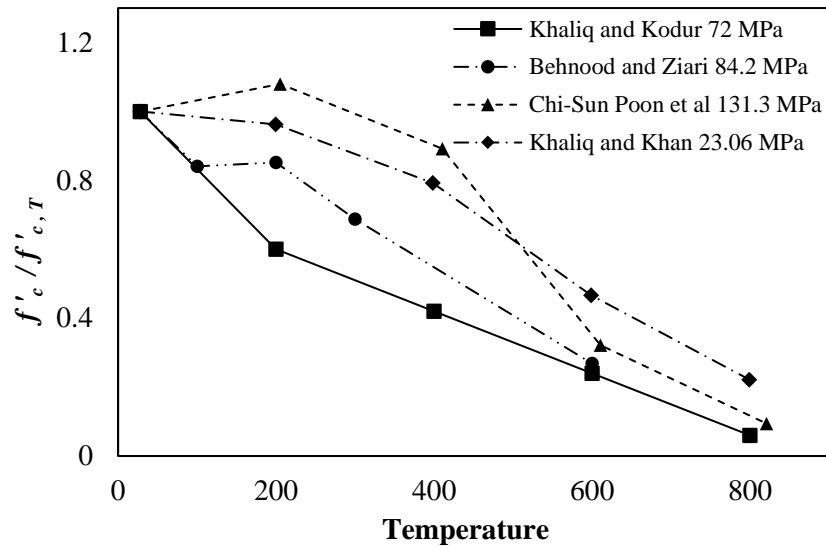
Fig. 1.1 Loss Compressive strength of concrete with increase in temperature of HSC and NSC
(Behnood and Ziari 2008; Khaliq and Khan 2015; Khaliq and Kodur 2012; Poon et al. 2003)

1.4   Research objectives and significance

The primary objective of this research program is to study the fire behavior of Air Entrained High

Strength Concrete (AEHSC) in terms of mechanical strength. The main objectives of this study

are

- To investigate loss in mechanical properties of air entrained HSC

- To study the effect of air entrainment on spalling behavior of concrete

- To visualize the cracking pattern produced and color change due to fire in AEHSC

- To carry out quantitative analysis of air voids on the fire behavior, by varying the amount
  of entrained air in concrete mixes

18

- To study the microstructure of air entrained HSC and non-air entrained HSC by Scanning Electron Microscopy (SEM) and by comparison of both, figure out the role of air voids of fire behavior

1.5 Research significance

The effect of elevated temperature on the mechanical, microstructure, thermal and permeability properties of both HSC and NSC is well understood and enough data of tests is available in the literature. There exist mathematical models to predict the fire behavior of concrete in several researches as they are given for by Phan and Carino (2003) and for thermal properties by Kodur and Khaliq (2010). However no data exist for fire properties of AEHSC for both unstressed and residual fire scenarios. In this research program mechanical properties of high strength AEC are studied.

1.6 Thesis layout

This thesis is subdivided into 5 chapters.

Chapter 1 "Introduction" is preliminary chapter which explains the significance of AEC, HSC and its behavior under fire, research objectives, significance, and thesis overview.

Chapter 2 "Literature Review" describes the previous literature and focuses on the previously done related researches in detail. The brief literature review includes the effect of fire on mechanical properties and spalling of HSC and air entrainment in super plasticized mixture.

Chapter 3 "Experimental program" discusses the test procedures and methodology. The target temperature, heating rate, specimen size, and equipment used in this study are described in this chapter.

Chapter 4 "Results and discussions" represents the test results, observations, and discussion on results.

Chapter 5 "Conclusions and recommendations" covers the concluding remarks made after this study along with related future research program.

<div align="right">

CHAPTER 2

</div>

<div align="center">

LITERATURE REVIEW

</div>

2.1   General

Extensive research with increasing knowledge of materials engineering specially in the area of concrete technology, has produced different types of concrete. One type of concrete cannot fit in all the environmental or loading conditions, every type of concrete is specialized in performance in its own environmental and loading condition. HSC is used where loads coming on the structure are greater than regular loads. It finds its applications in columns of frame structures, pre-stressed concrete members, concrete arches, girders and bridges. Similarly, AEC is specialized in water freezing weather conditions and is more durable against freeze-thaw cycles than conventional concrete. Combining air entrained and high strength concretes is not a routine practice because a number of authors believe that there is no need of entraining air in HSC to make it durable (Aıtcin 2003; Kriesel et al. 1998; Pigeon et al. 1991). Hence, combining HSC and AEC is not very common, furthermore entrainment of air in concrete formulation decreases the strength of concrete so concrete material engineers avoid entraining air in HSC. Although entraining air in concrete improves its workability, so for the same workability water content of AEC can be reduced which imparts strength in the mixture so the strength reduction due to air entrainment can be offset. However, in literature there is no study available which covers the fire properties of air entrained high strength concrete.

2.2   Entraining air in high strength concrete

Entraining air in HSC requires special attention, because HSC formulations are always superplasticized by certain superplasticizers. Using Air Entraining Agent (AEA) in this superplasticized formulation usually causes chemical incompatibility. So, air entrainment in HSC needs a vital knowledge about nature of chemical admixtures being used and their behavior with other chemical admixtures. Commercially available SPs often contain some anti-foaming agents like tri-butyl phosphate to remove air voids caused by inadequate polymerization of condensate, which is undesirable. Moreover, these anti-foaming agents are also used to increase the shelf life of superplasticizers. According to Siebel (1989) this antifoaming agent disturb the stable air void system in hardened state which is essential for freeze thaw durability of concrete. This state of the art report states that chemical formulations of AEAs and SPs have some compatibility issues and air void system introduced with hollow plastic microspheres of sizes (10-50 micro meters) are more suitable than using AEAs. Conclusion drawn based on the tests conducted by Mielenz and Sprouse (1979) is that in superplasticized mix amount of AEA is reduced to achieve a certain level of air percentage in fresh state but air percentage in harder state is lowered and also the size of air voids is increased by using AEAs with SPs. Also the average chord length (l), which is defined in ASTM C457/C457M-12 (2012) as "the length of chord formed by the transection of the air voids by the line of traverse" and is specified as 200 μm (spacing factor , (L)) for better freeze- thaw resistance by Powers and Willis (1950), is disturbed and is increased. According to MacInnis and Racic (1986), adding SP in fresh state of concrete which already contains some AEA causes decrease in air content, increase in spacing factor and decrease in air void surface areas. Litvan (1983) also observed the disturbance in air void system of air entrained superplasticized pastes. Based on all above results and those obtained by themselves Baalbaki and Aitcin (1994) concluded

that it cannot be generalized that which AEA will suitable in superplasticized paste. The results obtained from each researcher are specific for their own type of chemical formulation used.

Moreover, the chemical characterization of SRM being used in concrete mix is also essential. The carbon particles which remain unburnt in the SRM during its preparation adsorb AEA making it inactive, as a result higher amount of AEA is needed based on the amount of carbon present as observed and stated by Freeman et al. (1997). The amount of carbon can be checked by simple LOI (Loss on Ignition) test but Freeman et al. (1997) also stated that not only the amount of carbon effects AEA activity but also type of unburnt carbon and its microstructure do. Although this statement was given after the tests performed on Fly Ash but it can be fit on any SRM containing unburnt carbon. Gebler and Klieger (1983) tested on different classes of fly ash according to ASTMC618-08a (2008), and was unable to generalize the results by saying that air void stability in concrete paste system depends on numerous factors like organic impurities and unburnt carbon in fly ashes etc. Gebler and Klieger (1983) also stated that current ASTM specifications covering quality of fly ash are not adequate to predict its behavior of entraining air. Gebler and Klieger (1983) focused on new needs of specifications regarding performance tests. The durability of slag blended cement in resisting freeze thaw cycles is also not satisfactory as shown by Giergiczny et al. (2009). Giergiczny et al. (2009) mentioned that decreased durability of slag blended cement is due to increase in air voids spacing factor and decrease in specific surface of voids. The detailed test program including almost all the factors which are likely to disturb the air void stability was carried out by Pigeon et al. (1989) and Plante et al. (1989), these factors included silica fume addition at different percentages, type of mixing concrete ingredients, type of cement and superplasticizers with different AEAs.

The SPs used by them were modified lignosulfonate + naphthalene (L), naphthalene based type (N), melamine based type (M) and a solid melamine based type and AEAs used were Vinsol resin based (VR), sulfonated hydrocarbon (SH) based and synthetic detergent (SD) based. Based on different permutations and combinations of cement type (based on Alkali percentage), AEAs and SPs, Fig 2.1 can be plotted against average chord length of air voids and alkali percentage in cement and Fig 2.2 can be plotted against specific surface. Specific surface (α) is defined as the surface area of the air voids divided by their volume in ASTM C457/C457M-12 (2012). Lignin based SP results are not plotted because its commercial use is very less also the results of Vinsol Resin based AEA are not plotted because due to its instability.
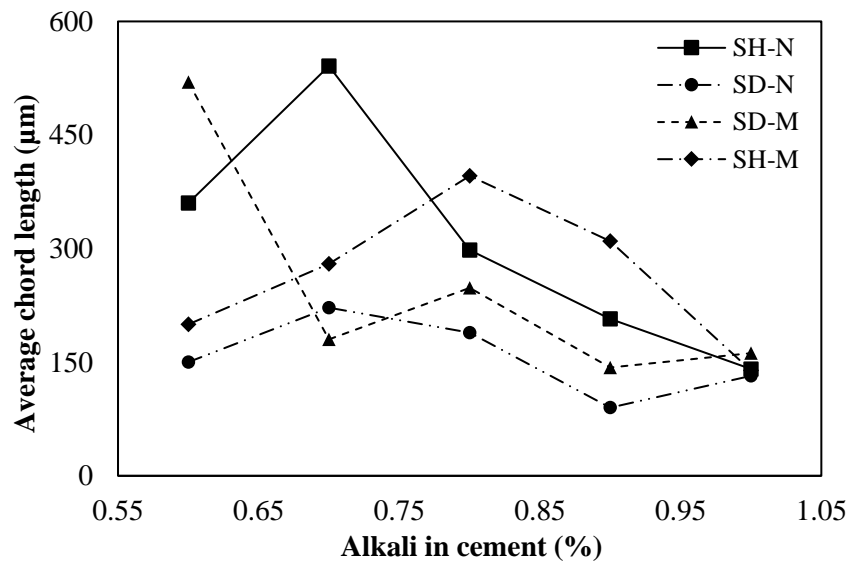
Fig. 2.1 Plot showing compatibility of AEAs and SPs based on average chord length
(Pigeon et al. 1989)

It can be concluded from graphs that based on average chord length the most stable combination is of Synthetic Detergent (SD) based AEA when used with Naphthalene (N) based SP along varying degree of Alkali percentage. Pigeon et al. (1989) also showed that silica fume has no effect on entrainment of air, neither in fresh state nor in hardened state. Hence using silica fume for

24

pozzolanic reaction, synthetic detergent based AEA and Naphthalene based SP will produce stable air void system in concrete.
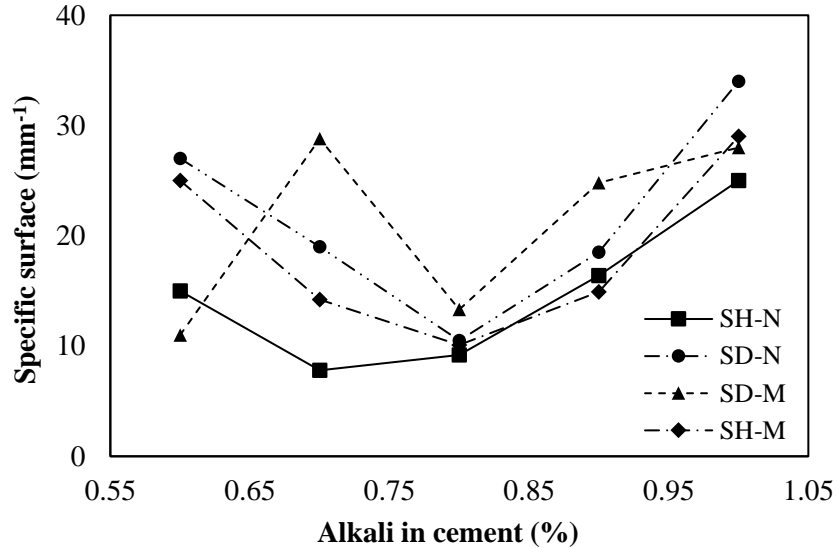
Fig. 2.2 Plot showing compatibility of AEAs and SPs based on specific surface
(Pigeon et al. 1989)

2.3 Material properties of high strength concrete at elevated temperature

Critically viewing at the literature, it can be seen that HSC at elevated temperature behaves differently from NSC in two ways (Phan and Carino 1998).

a) Higher magnitude of strength loss induced by elevated temperature than NSC in a temperature range of 100°C to 400°C.

b) Failure due to spalling of concrete with an explosion at rapidly increasing rate of temperature which is again in contrast with NSC.

The rate of strength loss with increase in temperature and explosive spalling are dependent on different test variables. Some of them are combination of time of application of load and heating scenario (stressed, un stressed and unstressed residual) (Phan and Carino 2002), initial moisture content of the specimen before fire testing (Chan et al. 1999), water-cementitious ratio (w/cm),

sand ratio, quantity of silica fume and its ratio (Bastami et al. 2011), heating and cooling rate (Luo et al. 2000), Aggregate type (light weighted or normal weighted) and polypropylene addition (Phan 2002). Since there is lack testing standards when fire behavior of concrete either HSC or NSC is to be studied. Different authors use different testing parameters but generally for HSC rate of heating concrete specimen is kept to (2°C-5°C)/min and cylinder size of 200mm height x 100 mm diameter is used (Hoff et al. 2000) , (Poon et al. 2004) and (Cheng et al. 2004) but different sizes are also used by some different researchers like 300mm x 150 mm used by (Husem 2006).

2.4   Testing method based on loading and heating regime

As far as fire behavior is concerned there are total three different scenarios of applying load and temperature namely Stressed, Unstressed and Residual.

In the stressed test condition load of magnitude which is 40% of member capacity is applied in pre-heating stage of test. The member is heated at a given heating rate up to the desired temperature after which the temperature is kept constant and is prevented to further increase in temperature. The remaining load is then applied with the desirable rate as shown in Fig 2.3(a). To perform test under this loading and heating regime, a sophisticated assembly of furnace and loading machine is needed i.e. sample is placed in the furnace while load is being applied on it. It is a complex system and not available commonly in structure engineering laboratories as special arrangements are required. The laboratories specially established to study the fire properties of structures mostly are equipped with this facility. This loading and heating regime truly depict the actual scenario of structures under fire event. The second testing scenario is unstressed test conditions. Under this condition, the specimen or member is not loaded in preheating conditions.
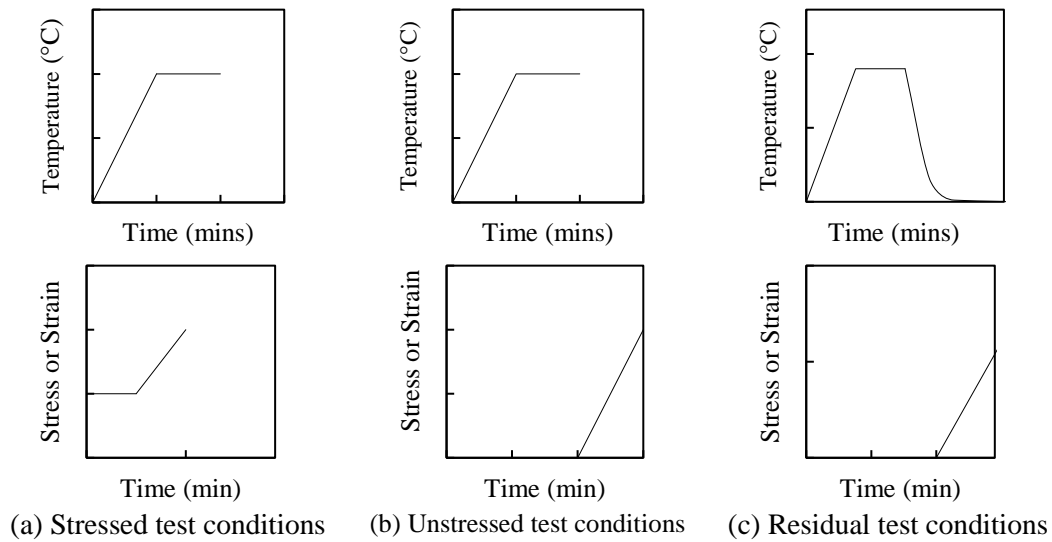
Fig. 2.3 Loading and heating pattern for stressed (a), unstressed (b) and residual test conditions (c)

In contrast to stressed method, the member or specimen is kept free from any loading and heating is applied at desired target rate up to the given temperature. The temperature is then kept constant and load is applied at a desired rate up to the failure of the structure. This heating and loading regime does not truly depict the actual structural conditions under fire. This testing condition finds its importance due to unavailability of stressed test condition equipment. The results obtained from unstressed test conditions although different from stressed conditions in magnitude but they follow the same trend and the structure under fire behave in a similar fashion in both these testing conditions. This testing and heating regime is shown in Fig 2.3(b).

In residual test conditions the member or specimen is heated at a desired rate up to certain temperature and then cooled down. When the temperature of the member or specimen is in equilibrium with ambient conditions, then member or specimen is loaded up to failure. The cooling regime in this test conditions also affects the test results (Luo et al. 2000). This loading and heating regime is shown in Fig 2.3(c). Testing specimens or members through this loading and heating

regime is most simple among all conditions. Despite of being least accurate model of actual loading scenario this test regime is frequently used due to its ease of high temperature test execution and simplicity. This is the reason that, most of the test data available in literature pertains to residual test conditions. The compressive strength of member is highly dependent on the testing scheme adopted. As shown in Fig 2.4, the results obtained from unstressed and stressed test conditions although differing in magnitude but are following the similar trend when compared to residual testing regime. The heating rate of air in the furnace chamber was 5°C/min. The details of mixture regime are represented in Table 2.1.

Table 2.1 Mix Regime of concrete used in plotting Fig 2.4

Ingredient	Quantity
Cement, kg/m^3	596
Water, kg/m^3	133 (0.33 water-powder ratio)
Coarse Aggregate, kg/m^3	846
Fine Aggregate, kg/m^3	734
Silica Fume, kg/m^3	66 (10 % of total powder)
28-Days Compressive Strength (MPa)	66.0
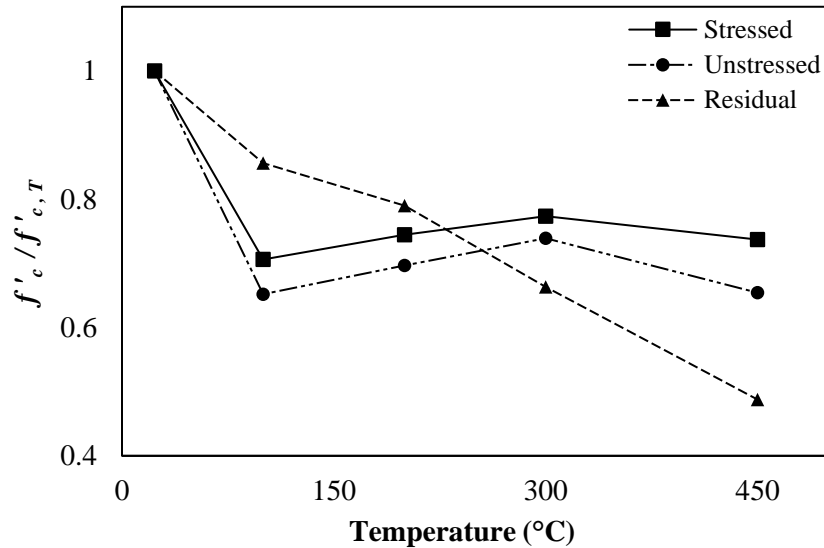
Fig. 2.4 Loss of compressive strength of HSC with increase in temperature under various loading and heating regimes

(Phan and Carino 2002)

28

2.5   Spalling

Spalling due to fire is said to be occurred when the layers or pieces of concrete are observed to break or observed to get separated sometimes with an explosion, when concrete structure (especially HSC) is exposed to rapidly increasing temperature as observed in fire. The biggest threat to a structure from spalling is that it causes inner layers or core of concrete structure to be directly exposed to fire. This exposure causes increase in temperature in core of concrete which is the main load bearing area and if steel reinforcements are also coming in the vicinity of thermal exposure then strength degradation in reinforcements starts to develop and the fire resistance of the whole structure diminishes rapidly and ultimately collapse of the structures occurs which was initiated by just spalling. Occurrence of fire induced spalling in NSC is rare. Sanjayan et al. (1993) captured the spalling behavior of HSC and NSC by measuring the weight of concrete structure with respect to time or temperature (because temperature was increasing with time) as shown in Fig 2.5.
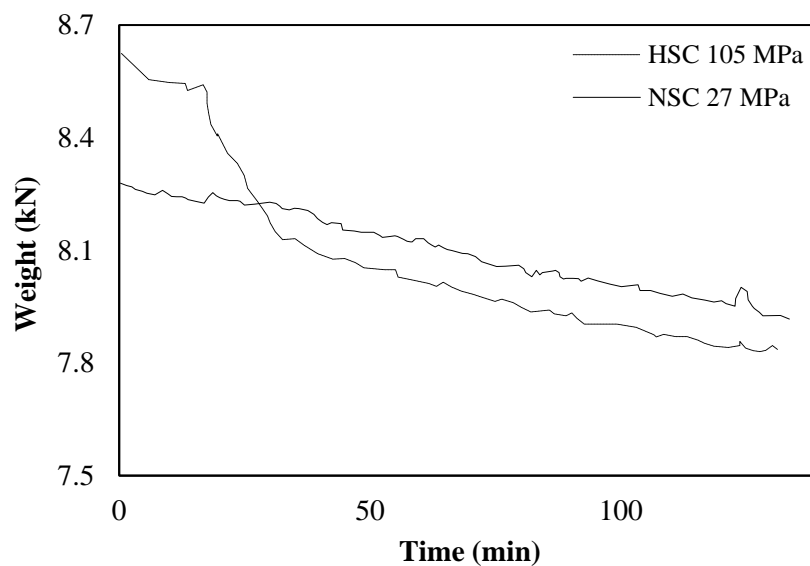
Fig. 2.5 Mass loss measured with increasing time and temperature for NSC and HSC
(Sanjayan et al. 1993)

As it is clear from the above Fig 2.5, at time of almost 17 minutes there is a sudden drop in weight of the structure which corresponds to spalling in HSC confirming that HSC is more prone to spalling than NSC. Phan (1996) observed that spalling observed in concrete due to fire is of explosive nature. Table 2.2 shows the studies on explosive spalling by various authors. From Table 2.2 it is clear that spalling is not always observed when HSC is subjected to elevated temperature. Although, there exists some factors which increase the probability of spalling. These factors can also be independent or inter dependent. From above Table 2.2 it can also be seen that chances of explosive spalling are highest in those mixes which are produced with silica fume.

To prevent spalling in concrete, it is necessary to have the complete knowledge of its occurrence. Without knowing the mechanism of spalling and its dependencies its prevention is difficult. In literature, explanations having different mechanisms of spalling are present. The contradiction arises possibly because there are so many factors upon which the spalling depends. Moreover, these factors are also inter-dependent on each other. According to Kodur (2000), there are two basic theories given by different researchers which explain the spalling behavior of HSC. Which are

a)   Internal Pore Pressure

b)   Release of thermal stresses

2.5.1 Internal Pore Pressure

Due to its very low permeability, when HSC is exposed to fire the water vapors are unable to find the route to escape from the concrete surface. This hindrance due to very low permeability builds up pore pressure within the concrete.

Table 2.2 Spalling in concrete at elevated temperatures reported by various authors

Test Program	Compressive Strength (MPa)	Mix Regime Characteristics	Specimen Size	Heating Rate	Spalling Temperature
(Phan and Carino 2002)	98[1],88[2],75[3]	(w/cm = 0.22, 10%SF)[1] (w/cm = 0.33, 10%SF)[2] (w/cm =0.33)[2]	200mm x 100mm Cylinder	5°C/min	(450°C)[1] (600°C)[2] (600°C)[3]
(Xiao and Falkner 2006)	83.3[1],109[2]	(w/cm=0.3, 40%GGBS)[1] (w/cm = 0.25, 10%SF)[2]	100mm x 100mm x 100mm Cubes	ISO-834	(500-600°C)[1] (800-900°C)[2]
(Chen and Liu 2004)	82.1	w/cm = 0.23, 10%SF	100mm x 100mm x 100mm Cubes	10°C/min	400°C
(Phan 2008)	75.3	w/cm = 0.23, 10%SF	200mm x 200mm x 100m Blocks	5°C/min	600°C
(Behnood and Ghandehari 2009)	85	w/cm = 0.30, 10%SF	102mm x 204mm Cylinders	3°C/min	No Spalling
(Chan et al. 2000)	97.3	w/cm =0.32, 10%SF&25%FA	100mm x 100mm x 100mm Cubes	(5-7)°C/min	No Spalling
(Kodur et al. 2003)	75.5	w/cm=0.22, 10%SF	100mm x 200mm	2°C/min	No Spalling

At 300°C, Pressure reaches up to 8 MPa which exceeds the tensile capacity of concrete (generally not more than 6 MPa). Thus causing chunks of concrete to fall off from the surface which can be of explosive nature depending upon concrete and fire characteristics (Anderberg 1997).

2.5.2   Release of Thermal Stresses

According to analysis done by Bazant (1997), the explanation of spalling due to pore or vapor pressure development is just a weak point. The actual phenomenon which causes the explosive spalling of concrete is that when concrete surface gets direct exposure to fire, expansion of hotter region occurs which is restrained by the neighboring concrete thus causing thermal stresses in hotter region. The release of energy stored due to thermal stresses is the main reason of spalling which is of explosive nature. This release needs to be analyzed through fracture mechanics.

According to Bazant (1997), the pore pressure built up mechanism just acts a trigger for spalling and not the main cause of it. To prevent the spalling to occur, the most widely accepted method and which is used frequently is the use of polypropylene fibers in concrete. Concrete specimen casted with and without polypropylene fibers by keeping all the characteristic same, expose off the effectiveness of these fibers. Similar type of testing was performed by (Han et al. 2005) and observed that polypropylene is very efficient tool to cope against spalling. The test results are tabulated in Table 2.3.

Table 2.3 Effect of polypropylene fibers on risk of spalling (Han et al. 2005)

w/cm	PP fiber (% of total volume)	Specimens		
		A (Metal Fabric)	B (Glass Fiber)	C (Carbon Fiber)
0.3	0	Spalled	Spalled	Spalled
	0.05	No Spalling	No Spalling	No Spalling
	0.1	No Spalling	No Spalling	No Spalling
0.4	0	Spalled	Spalled	Spalled
	0.05	No Spalling	No Spalling	No Spalling
	0.1	No Spalling	No Spalling	No Spalling

The mix with w/cm ratio of 0.30 was prepared with 20% Fly ash. Concrete cylinders were confined with metal fabric, glass and carbon fibers. The specimens were tested under standard ISO-834 fire curve. It can be seen from the Table 2.3 that only factor which is preventing concrete cylinders to spall is polypropylene fibers presence. The detailed explanation about how PP fibers decrease the probability of spalling is given by Kodur (2000). The reason of improved behavior is of course the permeability. The fiber reinforced concrete possess more permeability than concrete with similar mix regime without fibers by a factor of 4. Thus permeability is the reason of improved performance against spalling.

2.6 Compressive strength:

Since compressive strength of concrete is considered to be its vital property so concrete is manufactured and used just for its good performance in compression. In present literature there is no such study available which covers the fire behavior of air entrained concrete even for normal strength. So, strength loss with increase in temperature for HSC and NSC is shown and compared. HSC differs from NSC in two ways. First of them is reduction in strength at higher rate with temperature when compared to NSC (Fig 1.1) and the second one is more chances of explosive spalling. The behavior of HSC is also shown in Fig 2.4 before.

2.7 Tensile strength

The explosive spalling behavior of silica fume based HSC is controlled by its tensile strength. The reason is that at temperatures greater than normal or routine temperatures, internal pore pressure is built within the concrete which generates tensile stresses in concrete and when these stresses exceed the tensile strength of concrete, spalling takes place. American Society of Testing Materials (ASTM) gives three independent methods to measure the tensile capacity of concrete (ASTMC78/C78M-10 2010), (ASTMC1583/1583M-13 2013) and (ASTMC496-11 2011).

Comparing data of split tensile strength of HSC and NSC reveals that just like compressive strength, split tensile strength is also dropped more rapidly in case of HSC than NSC.

All three test programs of Table 2.4 are for same specimen size which is 200mm x 100mm. It is clear from the Fig 2.6 that tensile strength of HSC follows same trend as compressive strength. Drop in tensile strength is more for HSC than for NSC.

Table 2.4 Mix regime details of Fig 2.6

Authors	Mix Regime	Mix Characteristics	28-Days Compressive strength (MPa)	28-Days Tensile strength (MPa)	Loading and Heating Pattern
(Khaliq and Kodur 2012)	HSC-1	w/cm = 0.25, 7% Silica Fume of total powder, cement content = 560 kg/m3	81	4.6	Unstressed
(Khaliq and Kodur 2012)	HSC-2	w/cm = 0.32 , 6% Silica Fume, 20 % Fly Ash and 11% Slag of total powder, cement content = 420 kg/m3	72	4.3	Unstressed
(Khaliq and Khan 2015)	NSC	w/c= 0.5, cement content = 410 kg/m3	23.06	3.26	Unstressed
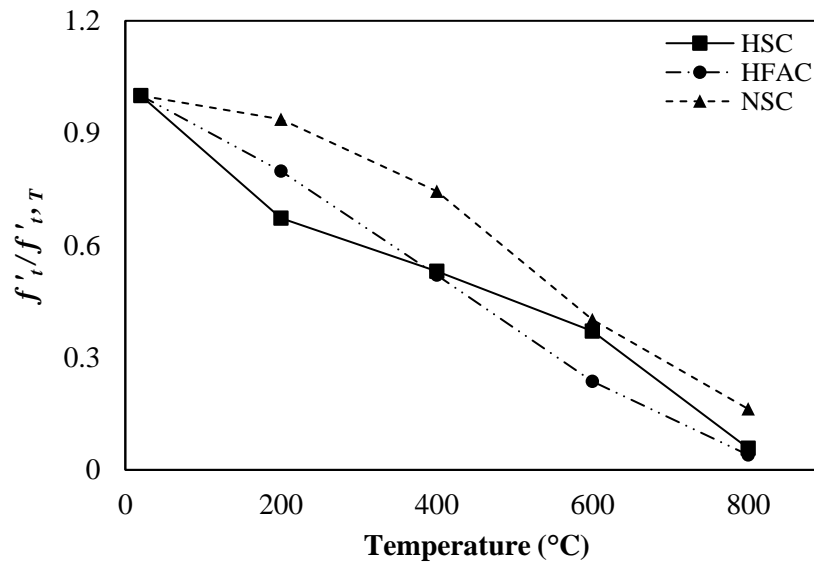
Fig. 2.6 Loss in Split Tensile Strength with temperature of HSC and NSC

2.8   Mass loss

Mass loss testing standards are given in ASTME1868-10 (2015). The concrete losses its mass or

weight by heating due to three different reasons. Which are

a)   mass loss due to free moisture

b)   mass loss due to spalling

c)   mass loss due to thermal instability of concrete ingredients

First is mass loss due to vaporization of free moisture present in the concrete pores. The mass loss due to this reason is mainly dependent on the amount of free water in pores and permeability. Increased amount of free water and enhanced permeability will result in higher mass or weight loss. Mass loss due to moisture is dominant in NSC, because NSC has higher w/c ratio and permeability than HSC. So mass loss due to moisture will be more in NSC as shown in Fig 2.8 (Kalifa et al. 2000). Two different concrete specimens of different strength and initial moisture are heated independently and their mass loss is recorded with increase in temperature.

The values of strength for NSC (M30) and HSC (M100) are 34.9 MPa and 91.8 MPa, respectively. M30 due to its lower strength, possess more initial free moisture and high permeability then M100. So mass loss measured against two different temperatures is more for M30 than M100 as expected. The second significant factor on which the mass loss depends is spalling of concrete from its surface. Despite of explosive spalling, there can exist localized spalling resulting in loss of small chunks of concrete with increase in temperature. The mass loss due to spalling will depend upon the factors causing spalling. Since spalling is critical only in HSC hence mass loss due to this factor will be dominant in HSC. As shown previously in Fig 2.5. The third major factor contributing mass loss is thermal instability of concrete ingredients mostly coarse aggregates. If the coarse aggregate portion is thermally unstable then it will result in more mass loss with increase in temperature irrespective to the strength of concrete (Lie and Kodur 1996)
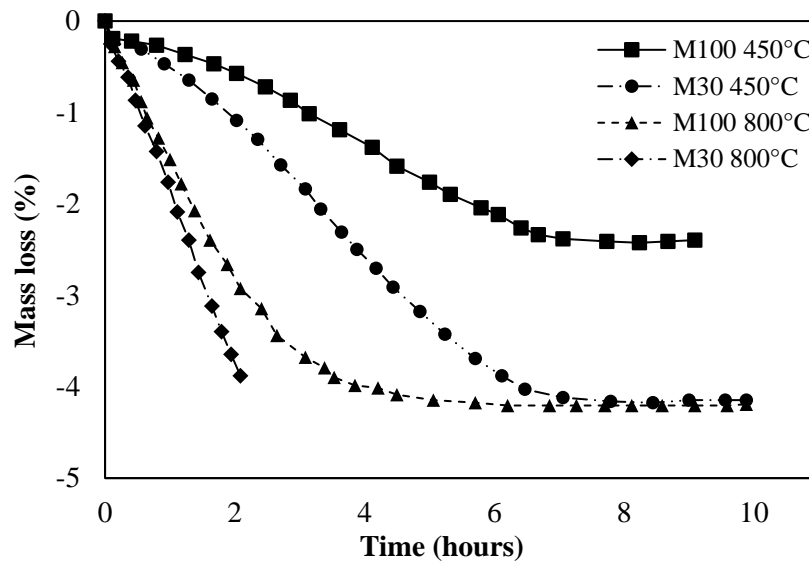
Fig. 2.7 Mass Loss of concrete with increase in time for NSC and HSC on 450°C and 800°C temperature

2.9   Elastic modulus

Elastic modulus is actually the measure of stiffness of a material or in other words it measures the deformation of material against applied loading. ASTM C469/C469M-14 (2014) covers the standards of testing procedure to determine the elastic modulus of concrete. To capture the response of stiffness of concrete there are three different types of modulus taken from the concrete stress strain plot

a)   Initial Tangent Modulus

b)   Secant Modulus

c)   Tangent modulus at any stress level

ASTM C469/C469M-14 (2014) gives the standards to calculate secant or chord modulus. Hence, only this type of moduli is calculated and discussed in this study. The starting point of that line is given as point of strain 0.00005 in ASTM C469/C469M-14 (2014) and ending point is given as

stress point of 0.4 f$_c$'. The expression given for elastic modulus (chord modulus) of normal strength concrete in ACI (Committee 2011) is $E_c = 4.73\ (f_c')^{0.5}$ MPa. Whereas, for concrete with higher strength this expression changes to $E_c = 3.32\sqrt{f_c'} + 6.9$ (Where E$_c$ is in GPa and f$_c'$ is in MPa) given in (ACI 1984) which is valid for f$_c'$ of 21 MPa to 83 MPa.

For ultra-high performance concrete (UHPC) this relation is given by (Kakizaki et al. 1992) is Ec=$3650\sqrt{f_c'}$ which is valid up to 140 MPa. It can be clearly seen from the above expressions that elastic modulus is a function of f$_c$'.Like compressive strength of concrete elastic modulus and stiffness against deformation of concrete is also dropped with increase in temperature. Also, trend of decrease in modulus of elasticity with temperature is different between HSC and NSC. Fig 2.8 is generated by combining the test results of Cheng et al. (2004) and Khaliq and Khan (2015). HSC having strength of 75 MPa, prepared with carbonate aggregate and tested in hot conditions (unstressed loading regime) are compared with NSC of strength 23.06 MPa with same aggregate type and testing conditions.
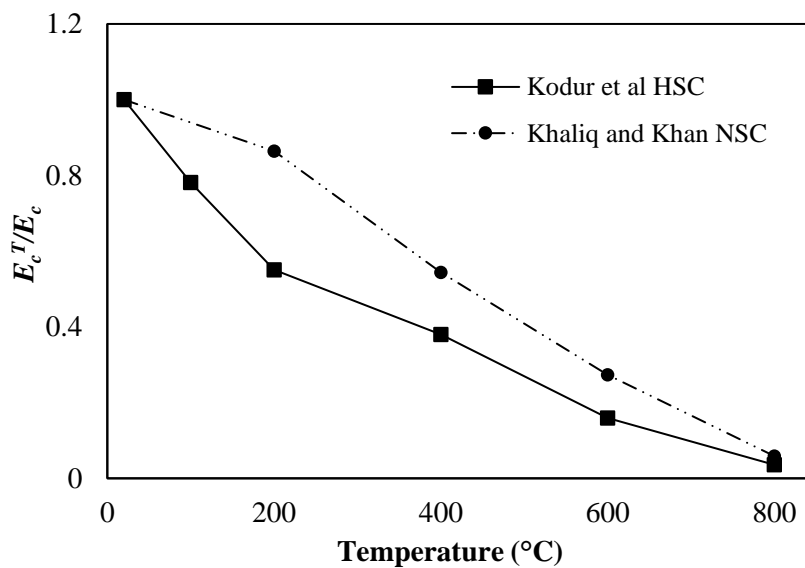
Fig. 2.8 Comparison of HSC and NSC with drop in elastic modulus with temperature

2.10   Stress strain response

When a concrete specimen is loaded in the machine and stress (usually compressive) is applied on it then plot of strain values against corresponding stress values is called as stress strain response. Stress strain response shows the whole picture of concrete specimen deforming with increase in load. With increase in temperature, a large increase in ductility of concrete is observed with decrease in compressive strength of concrete. Cheng et al. (2004) tested concrete specimens of HSC for their stress strain plots and observed the effect of steel fibers on the behavior of concrete when tested at elevated temperature. Fig 2.9 is plotted for HSC of strength 75.5 MPa. As it is clear from the above Fig 2.9 that peak stress or ultimate compressive capacity of concrete is decreasing with increase in temperature and strain at failure is increasing with increase in temperature.
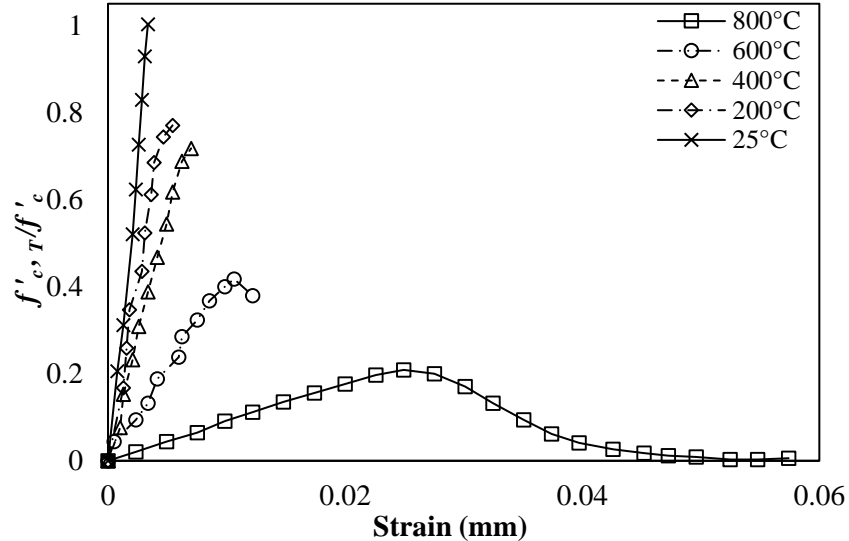
Fig. 2.9 Graph showing the change in behavior of stress strain plot of HSC with increase in temperature

(Cheng et al. 2004)

The difference is very less up to 600°C, but above 600°C large increment in strain values and decrement in stress values can be clearly noticed. Although these values are specific for a particular

mix regime of concrete, but all HSCs behave in a similar fashion when subjected to elevated temperature as similar trends can be seen in the test results of Lie and Kodur (1996). NSC also behaves in such a way i.e. increase in ultimate strain at elevated temperatures as shown in models of stress strain behavior of concrete at elevated temperature given by Harada et al. (1972). Furthermore, increase in ultimate strain due to high temperature in carbonate aggregate is higher than siliceous aggregate as shown by Cheng et al. (2004).

2.11 Microstructural changes causing drop in mechanical strength

In the concrete mix the main binding agent is calcium silicate gel which is the product of cement and water. Loss in its binding properties causes loss in mechanical strength of concrete. When the concrete specimen is heated at higher temperature the moisture present in calcium silicate gel is evaporated which as a result disturbs the van der walls forces present between aggregate and gel, Hence, bond between them is attenuated. Consequently the mechanical strength of concrete is decreased at 100°C and above (Lankard et al. 1971). Minor strength recovery is observed at 200°C which is believed to occur due to the general stiffness of calcium silicate gel or regain of the bond between aggregate and gel which is a result of evaporation of adsorbed moisture (Castillo 1987). The evaporation of adsorbed water depends upon the density of microstructure. Strength recovery between 100°C and 300°C is also attributed to rehydration of calcium silicate gel due to increase in temperature (Lie and Kodur 1996). The temperature which is in correspondence to the peak point in strength recovery phase is not fixed and it fluctuates depending upon the moisture content value and density of microstructure of concrete.

The temperature higher than 300°C causes disintegration of calcium silicate gel. Moreover, the aggregates expand at this temperature and calcium silicate gel shrinks due to evaporation of

39

moisture at 400°C and above (Georgali and Tsakiridis 2005; Janotka and Nürnbergerová 2005). This simultaneous expansion and shrinkage causes loss in bond between aggregate and gel at a larger scale. As a result large strength decrement is observed in high strength as well as in normal strength concrete (Benjamin 1962; Menzel 1943). In the limestone based coarse aggregates which are also used in this study, calcination of limestone aggregates is occurred at 600°C and above (Lie and Kodur 1996). Hence, a sudden drop in mechanical strength is observed due to calcination of coarse aggregates.

2.12   Air entrained concrete

2.12.1 General

Air entrained concrete is simply conventional concrete with intentionally entrained tiny air bubbles. It finds its applications in term of enhanced durability, improved workability and light weight concrete. In this section general behavior of air entrained concrete at room temperature is presented as there is no data available for AEC when subjected to elevated temperature. Despite of increase in durability of concrete by entraining air, there are other properties of concrete which are greatly affected by air entrainment. These are discussed in this section.

2.12.2 Strength and workability

The most important property of concrete when it is used as building material is its compressive strength which largely depends upon the density or porosity of concrete. Since, air entrained concrete effects the porosity of concrete and increases its porosity so it has negative effects on the strength of concrete.
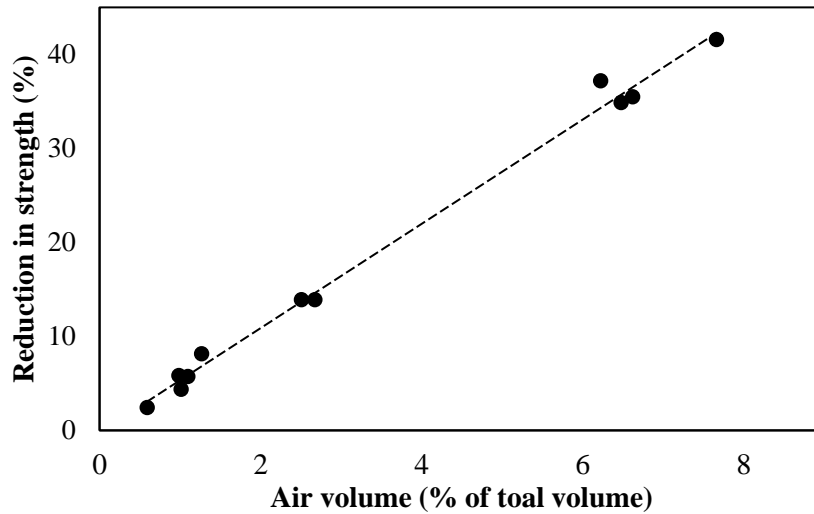
Fig. 2.10 Reduction in strength of concrete with increase in air quantity

(Wright 1953)

Increased quantity of air in concrete whether it is entrained intentionally or it is entrapped due to poor compaction increases the porosity of concrete in hardened state which further reduces the compressive strength of concrete. Fig 2.10 is plotted by examining strength reduction at different percentages of air for various concrete mixes by Wright (1953). The 28 days compressive strength and water-cement ratio for these mixes are 46 MPa & 0.45, 31 MPa & 0.55, 28 MPa and 0.62 and 19 MPa & 0.72. It can be further deduced from the above Fig 2.10 that 1% entrainment of air in concrete reduces strength of about 5.5%. This is also reported as a rule of thumb in (Mindess et al. 2003). Despite of lowering the strength of concrete air entrainment improves the workability of concrete. The reason of enhanced workability is due to the fact that air bubbles remain spherical due to surface tension and act as fine aggregates of very low surface friction. This phenomenon is called as ball bearing effect of air voids by Chia and Zhang (2007). This enhanced workability can be used to reduce the water content of concrete which results in improvement of strength. Hence, strength reduction by air entrainment can be offset by lowering the water content of concrete by the virtue of improved workability air entrained concrete. In Table 2.5, generated from work of

Chia and Zhang (2007) all other parameters were kept constant including fineness modulus of sand, the only variable was quantity of air.

Table 2.5 Workability of concrete mixes with varying air percentage (Chia and Zhang 2007)

Air Entrainment	Air Content	Density of fresh concrete (Kg/m3)	Slump (mm)
Non air entrained	4%	1860	35
Air entrained	6%	1835	140
	8%	1775	165
	12%	1665	150

Hence, at same slump or workability level water content can be decreased in the case of air entrained concrete and strength loss can be recovered.

2.12.3 Other strength related properties

Other strength related properties of AEC like splitting tensile strength, elastic modulus, stress-strain response and compressive toughness are not discussed or tested separately in literature. The reason of this is probably that AEC behavior for these properties will be just like non air entrained concrete of similar compressive strength.

2.13 Surface finishing of specimen before high temperature testing

In contrast to cubes casted by concrete, the cylinders casted with concrete will always have at least one surface which is quite rough and contains many undulations. If that surface is placed in compression testing machine in its natural form i.e. without its proper surfacing then stress concentration takes place at some areas leading to large errors in compressive strength. To avoid these types of errors in compressive strength, tolerance for surface planeness is given in ASTM C617/C617M-15 (2015).

There are several techniques which are being used to cope with these discrepancies. To cap the cylinder with gypsum or sulfur (in the case of HSC) according to ASTM C617/C617M-15 (2015) is most common among them. Sometimes, the unbonded caps are also used to avoid the time consumed in capping the cylinders with gypsum or sulfur according to ASTMC1231/C1231M-12 (2012). Both these above techniques are quite useful and accurate but their limitation is that these cannot be used in high temperature testing. To carry out the unstressed test i.e. testing the specimen in hot conditions is impossible by these two techniques because it is not possible to perform bonded capping in hot conditions. Moreover, when the specimen is heated at temperature as high as 800°C and unbonded caps are used before performing compression test then unbonded caps will definitely be damaged upon touching the hot concrete surface. That's why in most of the studies carried out by various authors these two methods are never used especially when unstressed tests are required to carry out. In replacement of these two techniques there is method used in almost all the studies covering high temperature testing. In that particular method the end surfaces of concrete cylinder not meeting the planeness criteria of (ASTM C617/C617M-15 2015) are ground and exactly flattened to meet the planeness criteria. The compressive strength test carried out by keeping the surface end conditions variable shows that results obtained by ground end are in accordance with the sulfur capped cylinder ends. Such comparison is shown in the following Table 2.6 which is derived from the experimental program of Carino (1994). From Table 2.6, it can be clearly seen that at almost all strength levels there is no difference between the compressive strength of surface ground specimen and sulfur capped specimen. Hence, in this study the surface ground technique is used.

Table 2.6 Comparison between compressive strength of sulfur capped cylinders and surface ground cylinders
(Carino 1994)

Design/Nominal Strength (MPa)	Average Compressive Strength of Ground Ends (MPa)	Average Compressive Strength of Sulfur Capped Ends (MPa)	Loading Rate (MPa/s)	Specimen Diameter (mm)
90	91.28	86.29	0.34	150
	88.12	86.14	0.14	150
65	69.16	68.81	0.34	150
	68.71	67.38	0.14	150
45	45.84	44.75	0.34	150
	44.77	43.64	0.14	150

<div align="right">

CHAPTER 3

</div>

<div align="center">

EXPERIMENTAL PRGORAM

</div>

3.1   General

Studying the behavior of air entrained HSC subjected to elevated temperature needs a detailed test program with various concrete mix regimes. The test program must include basic mechanical testing of concrete specimens including compressive and split tensile strength tests, stress strain plots, elastic modulus, compressive toughness, and mass loss. High strength air entrained concrete is discussed in details in the literature by various authors but there is no single series of tests available which covers the mechanical properties of air entrained high strength concrete under fire.

In order to understand the fire and spalling behavior of air entrained high strength concrete, basic mechanical tests namely compressive and splitting tensile strength test, stress strain response, elastic modulus, and mass loss are performed at temperatures of 23, 100, 200, 400, 600 and 800°C for both residual and unstressed test conditions. The details about test program and procedure, materials and mix regime are discussed in details in this chapter.

3.2   Preparation of specimens

3.2.1   Materials

The following materials are used in this study and are described below:

3.2.1.1 Cement

Ordinary Portland Cement (OPC) was used as a binder in this study. Its chemical composition obtained from X-ray fluorescence (XRF) technique is shown in Table 3.1.

Table 3.1 Quantitative analysis of OPC, Silica Fume 1 (BASF) and Silica Fume 2 (Sika) used in this study by XRF technique

Constituents	Mass Percentage (%)		
	O.P.C	Silica Fume 1	Silica Fume 2
CaO	79.0	1.8	1.3
Al_2O_3	13.82	--	--
SiO_2	5.8	96.98	89.24
Fe_2O_3	1.16	0.2	5.54
$ZnO+MnO+TiO_2$	0.22	--	0.31 (MnO)
K_2O	--	1	3.61

3.2.1.2 Fine Aggregates

Natural sand was used in this study which was obtained from Qibla Bandi Dam. Fineness modulus of the most of the sands of Pakistan is less than 2.4 because sands of Pakistan are quite finer. At the same workability value finer sand require more superplasticizer than coarser sand and in this study to prevent the usage of large volumes of Superplasticizer, coarser sand was specially arranged having fineness modulus of 2.7. The absorption of sand was 1.5%. The results of sand gradation and its comparison with ASTMC33/C33M-13 (2013) limits is given in Table 3.2 and Fig 3.1 below.
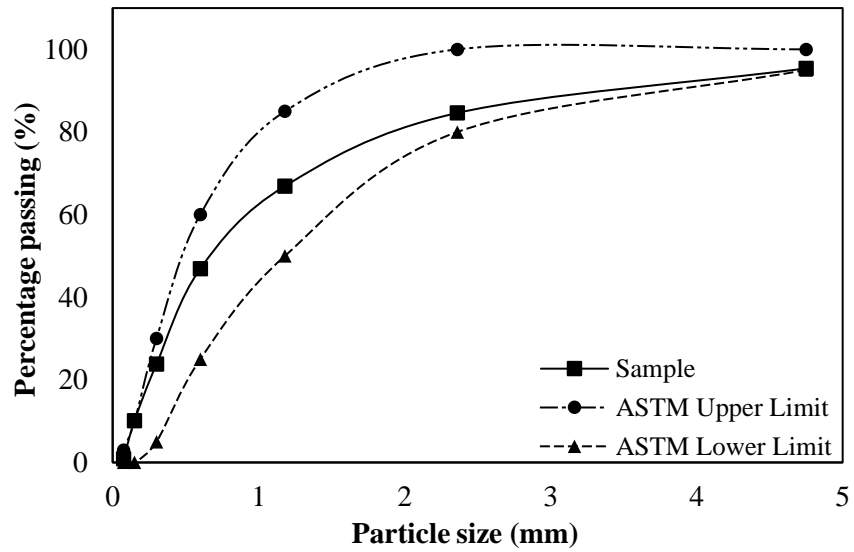
Fig. 3.1 Gradation of fine aggregates with ASTM bounds

Table 3.2 Gradation of fine aggregates and comparison with ASTM Limits

Sieve Number	Sieve Size (mm)	Weight Retained (grams)	Percent Retained (%)	Cumulative Percent Retained (%)	Percent Passing (%)	ASTM Lower Limit	ASTM Upper Limit
#4	4.75	46	4.6	4.6	95.4	95	100
#8	2.36	108	10.8	15.4	84.6	80	100
#16	1.18	177	17.7	33.1	66.9	50	85
#30	0.6	200	20	53.1	46.9	25	60
#50	0.3	231	23.1	76.2	23.8	5	30
#100	0.15	137	13.7	89.9	10.1	0	10
#200	0.075	92	9.2	99.1	0.9	0	3
Pan	0	9	0.9	---	---		
Total		1000	100				

3.2.1.2 Coarse Aggregates

Coarse aggregates used in this study were limestone based and were obtained from Margalla, Taxila. The maximum size was 9.5 mm. The gradation of aggregate in its natural state was not according to ASTM C-33, so a blend of different sizes was prepared to bring the gradation in between the ASTMC33/C33M-13 (2013) bounds. The final gradation after making blend of different sizes of coarse aggregate is shown in Fig 3.2.

Other properties of coarse aggregates and fine aggregates are tabulated in Table 3.3 below.
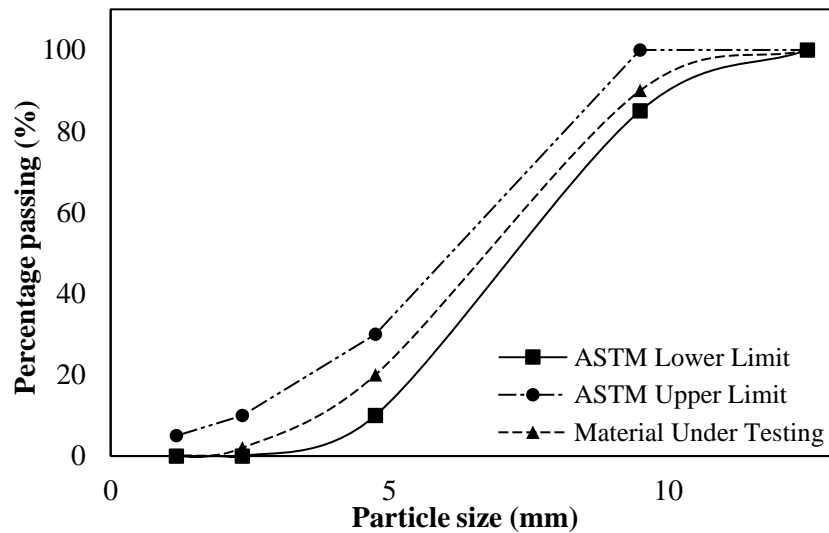
Fig. 3.2 Gradation of Coarse Aggregates with ASTM bounds

Table 3.3 Properties of aggregates

Sr No.	Property	Results
1	Bulk Specific Gravity of Sand	2.79
2	Absorption Value of Sand	1.50%
3	Fineness Modulus of Sand	2.723
4	Bulk Specific Gravity of Coarse Aggregate	2.65
5	Absorption of Coarse Aggregate	1.16%
6	Maximum Aggregate Size of Coarse Aggregate	9.5 mm
7	Dry-Rodded Bulk Density	1488 kg/m^3

Fig. 3.3 A view of crushing plant from coarse aggregate was arranged (Source: Maragalla)

3.2.1.3 Water

Potable water was used for mixing and curing of concrete.

3.2.1.4 Chemical and Mineral Admixtures

The mineral admixture or secondary raw material used was Densified Silica Fume having bulk specific gravity (BSG) of 2.241. It was chosen from two commercially available silica fume products. One was from BASF Chemicals (PVT) LTD and other was from Sika Chemicals (PVT) LTD. Chemical characterization of both products is shown in the Table 3.1 above. In the Table 3.1 Silica Fume 1 was manufactured by BASF Chemicals (PVT) LTD and Silica Fume 2 was manufactured by Sika Chemicals (PVT) LTD. Based on the quantity of SiO_2, which is the main pozzolonic agent, Silica Fume 1 was chosen from two. The Superplasticizer used was naphthalene

based second generation high range water reducer having BSG of 1.22. Its commercial name is RheoBuild® 850. The air entraining agent used was Synthetic Detergent based with BSG 1.064. Its commercial name was MicroAir® 720. All these admixtures were from BASF chemicals (PVT) LTD. This step of the research program i.e. selection of chemical admixture was most important and crucial because in this study air entrainment with limits of spacing factor and specific surface given by (Powers and Willis 1950) was intended. It is discussed in detail in Section 2.2. Shelf life of all admixtures is two years if stored according to manufacturer's recommendations. The details are given in Table 3.4 below

Table 3.4 Properties of admixtures
(ASTMC260/C260M-10a 2010; ASTMC494/C494M-15 2015; ASTMC1240-15 2015)

Admixture	Classification standards	Chloride and Nitrate content	Density (Kg/m^3)	Recommended Dosage [liters/100 kg of cement]
Super Plasticizer	ASTM C - 494 Type B,D and G	Nill	1220	(0.8-2)[1] liters/100 kg of cement (1.5-3)[2] liters/100 kg of cement
AEA	ASTM C – 260 EN 934-2 : T5	Chloride content <0.2%	1064	(0.04-0.4) liters/100 kg of cement
Silica Fume	ASTM C – 1240		2241	5-10% of cement

1 When used without silica fume

2 When used without silica fume

3.2.2 Mix Proportions

Total 4 different high strength mix regimes were prepared. Two of them were having entrained air whereas other two were non air entrained. For non-air entrained regimes, first mixture was having w/cm of 0.3 and second was having w/cm of 0.32. For air entrained regimes, both were having w/cm of 0.3. The difference between them was varying entrained air quantity. First air entrained mixture (overall third mixture) was having 4% entrained air whereas second air entrained mixture (overall fourth mixture) was having 8% entrained air.First mixture (NAEHSC1) and second

mixture (NAEHSC2) were prepared as control mixtures. Acronym NAEHSC# means Non Air Entrained High Strength Concrete where numeric (1 or 2) after last alphabet is used to distinguish between them. Third mixture (AEHSC4) was prepared to match the mixture characteristics of NAEHSC1 to compare the air entrained and non-air entrained high strength concrete with similar mixture composition. Fourth mixture (AEHSC8) was prepared to match the 28 days compressive strength of NAEHSC2 to compare the air entrained and non-air entrained high strength concrete with similar compressive strength. Acronym (AEHSC#) means Air Entrained High Strength Concrete, where numeric (4 or 8) after last alphabet represents quantity of air measured as percentage of total volume in fresh state. The mix details are given in the Table 3.5 below

Table 3.5 Details of concrete mix proportions

Components	NAEHSC1	NAEHSC2	AEHSC4	AEHSC8
Ordinary Portland Cement (Kg/m^3)	500	500	500	500
Silica Fume (Kg/m^3)	50	50	50	50
Water Content (Kg/m^3)	165	176	165	165
w/cm ratio	0.3	0.32	0.3	0.3
Coarse Aggregate (Kg/m^3)	1050	1035	1009	943
Fine Aggregate (Kg/m^3)	677	668	651	608
Super Plasticizer (mL/m^3)	9500	9000	8000	9000
Air Entraining Agent (mL/m^3)	--	--	1077	1280
Air (%)	1.5	1.3	4	8
Slump (mm)	95	100	105	130
Short Name	**NAEH-1**	**NAEH-2**	**AEH-4**	**AEH-8**

3.2.3 Mixing of Concrete Ingredients

Horizontal drum mixer (Fig 3.4) was used to carry out the mixing of concrete ingredients. The coarse aggregates were first added to the mixer with 25% mixing water. Then densified silica fume was added and mixing of about 3-4 minutes was carried out to convert it into slurry formation. After that fine aggregates were added and allowed to mix it for 2 minutes. Then cement was added with 50% water to the mixer and allowed to mix completely. After that remaining 25% water was

51

added in which superplasticizer was pre-mixed. In the end air entraining agent was added. Mixing were carried out according to (ASTM C192/C192M-16a 2016).

Fig. 3.4 Horizontal concrete mixture

3.2.4 Concrete Specimen Preparation

The freshly prepared concrete were placed into the steel molds in two layers with 25 blows per layer as given in (ASTM C192/C192M-16a 2016). The size of specimen were 200mm x 100mm (200mm height and 100 mm diameter). Top surface of freshly prepared concrete was finished by trowel. All the specimens were kept in the molds for 24 hours, after 24±4 hours the specimens were demolded and were kept in to the curing tank for 28 days under 95% humidity and 23°C temperature.

(a)   (b)

Fig. 3.5(a) Concrete specimens in fresh state

Fig. 3.5(b) Concrete cylinders of all the mixes in hardened state

Concrete specimens were ground from the ends to smoothen the surface and to meet the tolerance according to ASTM C617/C617M-15 (2015).

Fig. 3.6 Concrete specimens with ground ends

Compressive strength tests were performed on concrete specimens at 7, 14 and 28 days according to ASTM C39/C39M-16b (2016) at room temperature. Split tensile strength test was done according to ASTMC496-11 (2011) at 28 days. Results of these two mechanical properties are tabulated in Table 3.6(a) and Table 3.6(b).

Table 3.6(a) Compressive strength of concrete mixes at 7, 14 and 28 days at room temperature

Age of Concrete	Compressive Strength (MPa)			
	Mixture Designation			
Days	NAEH-1	AEH-4	AEH-8	NAEH-2
7	69.5	61	48.5	62.5
14	75.5	66	52	67.5
28	80	69.5	55	71

Table 3.6(b). Split Tensile Strength of concrete mixes at 28 days at room temperature

Mixture Designation	28 Days Split tensile strength (MPa)
NAEH-1	5.7
AEH-4	5.1
AEH-8	4.6
NAEH-2	5.1

3.3   Material property test

Mechanical properties tests namely compressive strength test, elastic modulus test, stress-strain curve and split tensile strength test were carried out after exposure to the desired temperature at a desired heating rate for all the four described mixes. Besides mechanical tests mass loss of each specimen were also calculated in residual conditions. The details of testing procedure and technique, testing equipment, testing variables and specimen fabrication is discussed in this section. The complete details of specimens tested at targeted temperature is given in Table 3.7.

Table 3.7 Details of specimens prepared to be tested at desired temperature

Sr No	Mix Type	Exposure Temperature (°C)	Compressive strength test	Elastic modulus test	Stress-strain curve	Splitting tensile strength	Remarks
Specimen Dimensions 200mm x 100mm							
1	NAEH-1	23	2	2	2	2	For unstressed and residual test conditions
		100	2	2	2	2	
		200	2	2	2	2	
		400	2	2	2	2	
		600	2	2	2	2	
		800	2	2	2	2	
2	AEH-4	23	2	2	2	2	For unstressed and residual test conditions
		100	2	2	2	2	
		200	2	2	2	2	
		400	2	2	2	2	
		600	2	2	2	2	
		800	2	2	2	2	
3	AEH-8	23	2	2	2	2	For unstressed and residual test conditions
		100	2	2	2	2	
		200	2	2	2	2	
		400	2	2	2	2	
		600	2	2	2	2	
		800	2	2	2	2	
4	NAEH-2	23	2	2	2	2	For unstressed and residual test conditions
		100	2	2	2	2	
		200	2	2	2	2	
		400	2	2	2	2	
		600	2	2	2	2	
		800	2	2	2	2	
Heating rate for the test specimens was 10°C/min							

3.4   Test specimens

A total of 40 specimens for each mix were prepared of the size 200mm x 100mm (Fig 3.7). There is very little data available in the literature which covers the fire response of concrete specimens of standard size used for compressive strength test i.e. 300mm x 150mm. So, smaller specimen size was chosen to compare the results with already tested sample results in literature.

Fig. 3.7 Cylinder size and dimensions

3.5   Fire loading characteristics

The results of specimens are largely dependent upon the characteristics of fire loading applied. There are two basic fire loading characteristics on which the results are dependent. These are heating rate and target temperature. Due to lack of high temperature testing standards available these two parameters were selected according to previously tested concrete specimens at elevated temperatures.

3.5.1 Target temperature

In the high temperature testing of concrete, the most frequently used temperatures on which the mechanical and thermal properties tests are carried out are 23°C (room temperature), 200°C, 400°C and 600°C. Because vapors play very important role in determining the fire response of concrete and vapors are created at temperature of 100°C. So, this temperature is very important especially for mechanical testing hence is added in this study.

3.5.1.1 Target temperature for residual test conditions

The target temperatures selected for residual test conditions in this study were 23, 100, 200, 400, 600 and 800°C.

3.5.1.2 Target temperature for unstressed conditions

In unstressed test conditions, the sample was required to test in hot conditions. Although, proper insulation material was used to cover the specimen still temperature drop was observed during transfer of sample from furnace to testing setup. Hence, this temperature drop was estimated and for unstressed test conditions specimen were heated beyond the target temperature so that during testing phase of specimen the core temperature was equal to the target temperature. The target temperatures selected for unstressed test conditions were also 23, 100, 200, 400, 600 and 800°C.

3.5.2   Hold time

When a concrete specimen is heated in the furnace then the temperature inside the air of furnace increases with the given rate. But the temperature of cylinder's surface and core always increases at a lesser increasing rate than the temperature of air of furnace. Conclusively, the temperature of air reaches at target temperature much earlier than cylinder. Hence, it becomes necessary to keep

the furnace temperature fixed at the target temperature for the time until the cylinder's core attains the target temperature, that time is called as hold time (or sometimes called dwell time). The method used in this study to calculate the hold time was adopted from Phan et al. (2001). Two thermocouples (Thermocouple is actually a set of wires which is used to measure temperature) were embedded in the cylinder, one in core and other on surface to track the temperature record. Thermocouples used in this study were type-K. The cylinder was drilled from one of the circular end, then thermocouple was inserted and cement paste was grouted in the drilled portion and it was then allowed to be harden. Similarly, the one thermocouple was embedded on the surface Fig 3.8(a). After that digital thermometer was attached with thermocouples to measure their temperature record Fig 3.8(b).

| (a) Thermocouple being embedded in concrete cylinder | (b) Thermocouples showing surface and core temperature of concrete specimen |

Fig. 3.8 Concrete cylinder attached with type-K thermocouple to capture temperature record

Then the thermocouple embedded cylinder was placed inside the furnace chamber and chamber was heated at a desired rate. The temperature track record was measured with respect to time for air entrained concrete only and was plotted as shown in the following Fig 3.9.
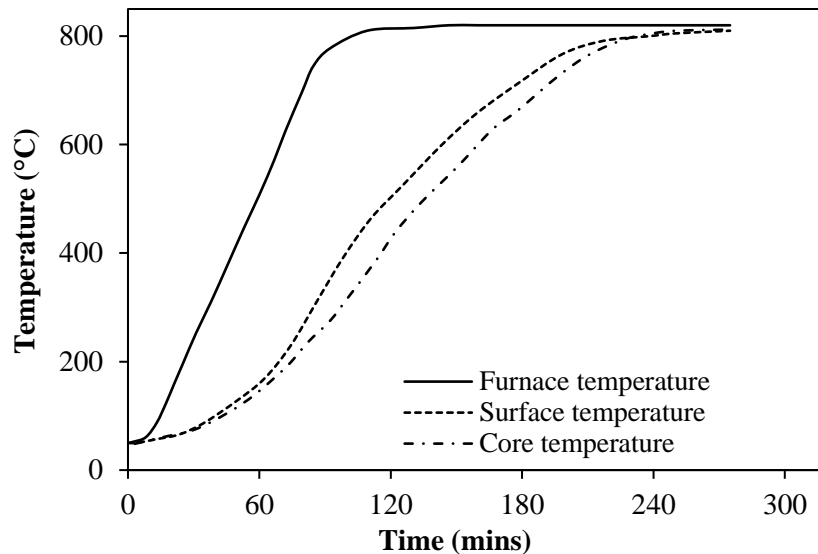
Fig. 3.9 Time temperature relationship of air entrained mixture concrete cylinder (AEH-4)

Thermal conductivity of concrete is largely dependent upon its porosity as highly porous concrete exhibits less thermal conductivity (Bouguerra et al. 1998) shown experimentally by (Kim et al. 2012). Since, air entrained concrete is more porous than non-air entrained concrete, So, hold time which is sufficient for air entrained concrete specimen will also be sufficient for non-air entrained specimen. It is clear from the above Fig 3.9 that core of cylinder takes 2^+ hours to attain the desired temperature. Hence, the hold time of 2.5 hours was given for all the mixes.

3.5.3 Heating rate

Heating rate is directly associated with spalling behavior of HSC specimens. The usual heating rate used by researcher is $(2°C – 5°C)$/min. But to the study the spalling behavior of concrete specimens a bit higher heating rate was selected which was $10°C$/min.

59

3.6 Test procedures

3.6.1 General procedure

The material property test at elevated temperature were carried out under two different test conditions i.e. unstressed and residual test conditions. These testing conditions are explained in Section 2.4.

3.6.2.1 Compressive strength test

After heating the specimen to the desired temperature up to stable thermal conditions, as defined in section 3.6.1, the specimen was wrapped in thermal jacket and was carried towards the compression testing machine in the case of unstressed test conditions and was allowed to cool down to room temperature in the case of residual test conditions. Because no testing standards are available in the literature which covers the high temperature compressive testing of concrete specimen, testing method of room temperature as described in ASTM C39/C39M-16b (2016) are followed to determine the compressive strength of concrete at desired temperature ($f_c',_T$). Sample was loaded with the loading rate of 0.2 MPa per seconds up to the failure of specimen with peak sensitivity of 50 kN. A concrete specimen during the compression test is shown in Fig 3.10 below. For temperatures other than room temperature one cylinder from each mix is heated and tested at higher temperature. If results were observed to be ambiguous or outliers, additional tests were done to confirm results. To compare the compressive strength of concrete specimen by unstressed test condition, relative unstressed/residual compressive strength was calculated by the following relation:

$$\text{Relative unstressed/residual compressive strength} = \frac{\text{Unstressed, residual strength at target temperature}}{\text{Room temperature strength}} = \frac{f_{c,T}'}{f_c'}$$

| Residual test conditions | Unstressed test conditions |

Fig. 3.10 Compressive strength test under action

3.6.2.2 Split tensile strength test

To measure the split tensile strength in unstressed and residual test condition (f_t', $_T$) specimen after stable thermal conditions (of desired temperature) were brought to steel bracket assembly with proper insulation to carry it towards the testing equipment without minimal thermal loss in case of unstressed test conditions and was allowed to cool down to room temperature in residual test conditions. ASTMC496-11 (2011) test standards were followed to test the specimen in room and desired temperature. Sample was loaded with the loading rate of 0.02 MPa per seconds up to the failure. Concrete specimen before and after split tensile test is shown in the Fig 3.11(a) and Fig 3.11(b).

$$\text{Relative unstressed/residual tensile strength} = \frac{\text{Unstressed, residual strength at target temperature}}{\text{Room temperature strength}} = \frac{f_{t,T}'}{f_t'}$$

<div align="center">

(a) Specimen before test   (b) Specimen after test
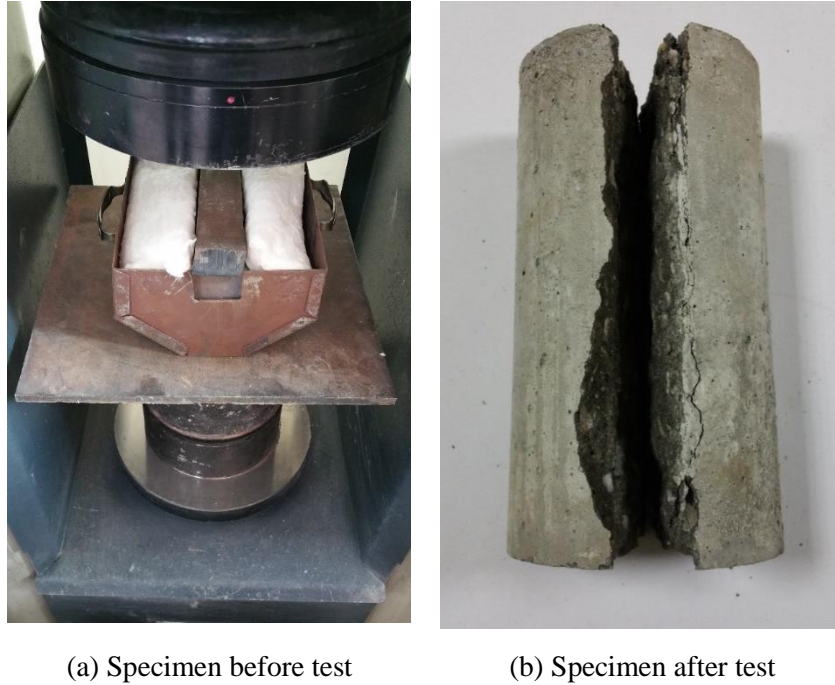
Fig. 3.11 Split tensile strength test

</div>

3.6.2.3 Stress-strain curve

To track the stress-strain response of concrete specimen, compression test was carried out data acquisition system. Fig 3.12(a) and Fig 3.12(b) below shows the setup for stress strain curve in compression under unstressed and residual test conditions, respectively. From load data acquisition system attached with compression testing machine and LVDTs, data of load and deformation was acquired, respectively. From load deformation response, stress strain curve was plotted at desired temperatures.

3.6.2.4 Elastic modulus

Stress-strain curve was used to evaluate the elastic modulus of concrete specimen at target temperatures. Chord modulus according to ASTM C469/C469M-14 (2014) was calculated nearest to 200 MPa by the equation 3.1 shown below:

$$E_c = \frac{S_2 - S_1}{\varepsilon_2 - 0.000050}$$

where,

E_c = Chord Modulus of Elasticity

S_2 = Stress corresponding to 0.4 f_c'

S_1= Stress corresponding to longitudinal strain of 0.000050

ε_2 = longitudinal strain corresponding to S_2

(a) Unstressed test conditions   (b) Residual test conditions
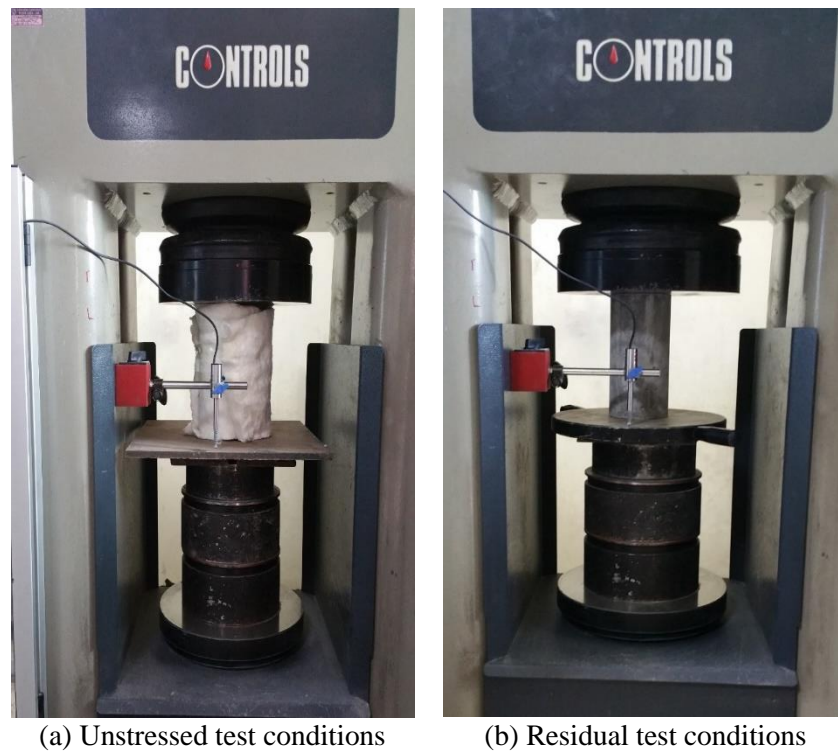
Fig. 3.12 Test setup for stress strain tests

3.6.2.5 Mass loss

To carry out the mass loss of concrete specimen, they were weighed before heating and after that specimen were heated to a targeted temperature and then were allowed to cool down to room temperature. After that specimen were again weighed on a weighing balance having least count of 0.001 grams. Relative mass loss measured at a targeted temperature was calculated from the following relationship.

$$M_{T,loss} = \frac{\text{Mass at target temperature}}{\text{Mass at room temperature}} = \frac{M_T}{M}$$

Derived from mass loss test, densities were also calculated and variation in density with temperature was also monitored.

3.7 General properties

Other properties of concrete specimen which are independent of loading and heating regime like crack propagation, spalling behavior and SEM analysis were also studied. To analyze the crack propagation some different techniques are used despite of just looking at the cracks with naked eye, because some hairline cracks are so small that it is quite cumbersome and difficult to analyze them with naked eye. Moreover, to present the difference of cracking pattern between two different concrete mixtures is also not that much effective when conventional techniques or procedures are adopted.

In this study two mixes NAEH-2 and AEH-4 were selected because of their equal room temperature compressive and tensile strengths. The cylindrical specimen were heated on each temperature including room temperature and then that specimen was cut along cross section into smaller pieces of height of nearly 40 mm. Then using high resolution cameras with enhanced zooming capabilities images were taken from different angles and then comparison was made between them.

While heating the specimen, some of them were spalled off with explosion. The record of their spalling was tracked and analyzed.

CHAPTER 4

RESULTS AND DISCUSSIONS

4.1 Introduction

This section covers the results obtained after test program described in detail in preceding chapter. The spalling characteristics, crack pattern and color change with increase in temperature are discussed first under the topic of general properties. Compressive strength, splitting tensile strength, stress strain response, elastic modulus, and mass loss are discussed after general properties under the heading of mechanical properties.

4.2 General properties

4.2.1 Explosive spalling/disintegration

Some of the concrete specimens when heated in the furnace chamber at a rate of 10°C/min spalled explosively. The results are plotted in the following table

Table 4.1 Description of specimen disintegrating/spalling explosively

°C	NAEH-1	NAEH-2	AEH4	AEH8
23	No Spalling	No Spalling	No Spalling	No Spalling
100	No Spalling	No Spalling	No Spalling	No Spalling
200	No Spalling	No Spalling	No Spalling	No Spalling
400	No Spalling	No Spalling	No Spalling	No Spalling
600	Explosive Spalling	Less Frequent Spalling	No Spalling	No Spalling
800	Explosive Spalling	Explosive Disintegration	No Spalling	No Spalling

NAEH-1 specimen spalled at a furnace/chamber temperature of 800°C, during the hold time of specimen almost after 20 minutes on average of 2 samples. The temperature of surface and core of cylinder was near 500°C and 420°C, respectively which is in accordance with Chan et al. (1999).

Specimen after spalling are shown in the following Fig 4.1. Spalling of this type was also reported by Han et al. (2005).

Fig. 4.1 Spalling of NAEH-1 mixture specimen

Likewise, NAEH-2 mix specimens spalled after 1.25 hours when temperature of 800°C is achieved in furnace/heating chamber. The temperature of surface and core of cylinder was measured to be 720°C and 650°C, respectively. The extent of spalling explosion of NAEH-2 was higher than of NAEH-1. The specimen image after spalling is shown in following Fig 4.2. Spalling of this type in HSC was also observed by Phan et al. (2001). No spalling or spalling with an explosion was observed in AEH4 and AEH8 specimen even at temperature as high as 800°C with a hold time of 2.5 hours. In the above Fig 4.2 the specimen placed besides the disintegrated one is air entrained specimen (AEH-4). Spalling was not observed in both mixtures as it can be seen from the following Fig 4.3.

Fragments of spalled non air entrained mixture specimen (NAEH-2)

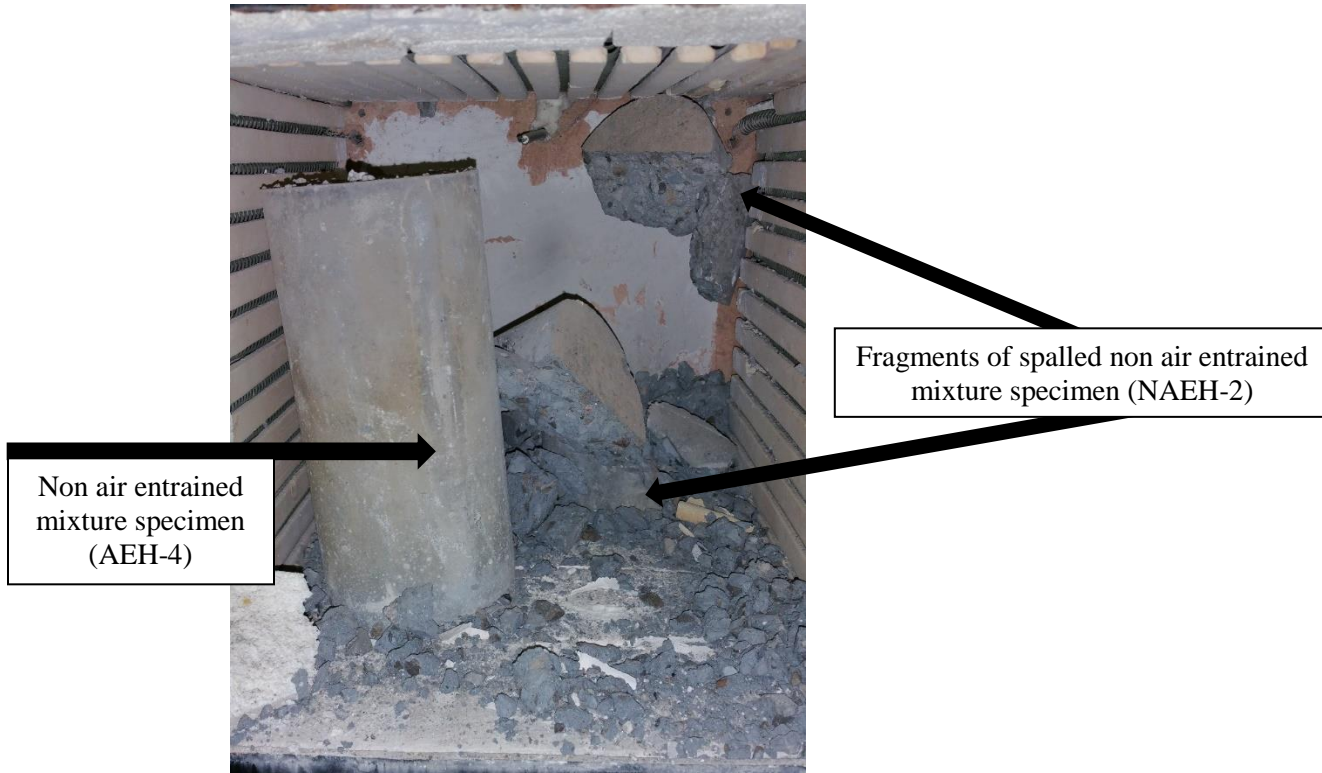Non air entrained mixture specimen (AEH-4)

Fig. 4.2 Spalling (explosive) of NAEH-2 mixture specimen

Fig. 4.3 Air entrained specimen after heating at 800°C

There are two main phenomenon which need to be explained. First is the spalling with explosion of NAEH-2 except just spalling although NAEH-2 possess lesser 28 days compressive strength with less denser microstructure and second is that chances of spalling or explosive spalling are significantly decreased when air is entrained in concrete mixture. The reason of the first phenomenon is that water content of NAEH-2 (176 kg/m^3) was higher as compared to NAEH-1 (165 kg/m^3). As a result, NAEH-2 had comparatively less strength but higher inner moisture. Owing to lesser strength and increased porosity NAEH-2 withstood more temperature than NAEH-1 before spalling (Chan et al. 1999; Xiao and Falkner 2006) but due to higher moisture and higher stored thermal energy the pore pressure produced in NAEH-2 mixture cylinders was much greater in impact than NAEH-1 which caused the NAEH-2 mixture specimen to disintegrate except just to spall of (Chan et al. 1999; Phan 2008).

In order to explain the enhanced resistance against spalling in the case of air entrained concrete, the relationship between porosity and explosive spalling/disintegration must be understood. In HSC, polypropylene fibers are usually mixed during its mixing stage, which at temperature of about 165°C melt and impart interconnected porosity in concrete, hence providing a pathway to the water vapors to escape except creating pore pressure and triggering spalling (Xiao and Falkner 2006; Zeiml et al. 2006). Porosity on concrete therefore provides resistance against spalling. Higher the porosity in concrete, lesser will be the chances for specimen to explode. Air entrainment in concrete increases its porosity in a similar fashion as polypropylene fibers do. The pore pressure produced inside the concrete cylinder due to vaporization is diminished due to presence of air bubbles connected to capillaries. As a result, explosive spalling/disintegration in air entrained concrete is prevented.

4.2.2 Analysis of cracks

Cracking pattern and cracks propagation is shown and discussed under this section. Concrete cylinders of mixtures AEH-4 & NAEH-2 only are selected for cracking analysis because of their similar 28 days compressive strength.

At high heating rates and at elevated temperatures, many factors such as dehydration of hydrated compounds, evaporation of various forms of water, differential thermal dilation of paste and aggregates, and thermal gradients lead to deterioration of microstructure resulting in excessive cracking in HSC (Fu and Li 2011). Table 4.2 shows the cracking pattern and cracks propagation in NAEH-2 and AEH-4 specimens with increasing temperatures. These two air entrained and non-air entrained HSC specimens are selected for crack development analysis based on their similarity in 28 days compressive strength. The figure shows that in NAEH-2 specimen the cracks appear and propagate below 400°C, whereas in AEH-4 specimen, cracking only appears before 800°C temperatures.

From the images in Table 4.2, it is evident that cracking initiated in NAEH-2 concrete between 200 to 400°C temperature as these are clearly visible in images at 400°C. The initial cracking is due to internal stresses induced by coupling of dehydration of C-S-H gel and thermal expansion of aggregates (Hertz 2005). As evident from Table 4.2, no such crack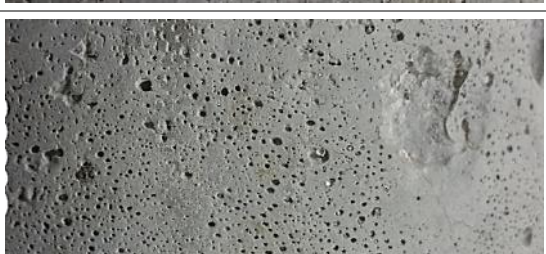ing is observed in AEH-4 concrete specimens, which demonstrates that distributed porosity provided by intentionally entrained air offers space for expansion of aggregates.

A higher amount of cracking is observed in NAEH-2 concrete at 600°C temperature (Table 4.2). This is attributed to decomposition of $Ca(OH)_2$, differential thermal dilations in paste and aggregates, and dehydration of C-S-H gel that occurs above 450°C. Conversely, such cracking is

absent in AEH-4 specimens, which shows that air entrained concrete withstands changes in microstructure at elevated temperatures.

Table 4.2 Thermal cracks comparison of air entrained and non-air entrained mixtures

Temp (°C)	Non air entrained HSC (NAEH-2)	Air entrained HSC (AEH-4)
100		
200		
400		
600		
800		

At around 650°C, calcination of $CaCO_3$ takes place, in which release of CO_2 also results in shrinkage and internal cracking in paste, further the rehydration of CaO to $Ca(OH)_2$ with moisture movement within the system causes expansive stresses on already deteriorating microstructure ending up with significant cracking. Similar deterioration also takes place due to high temperature thermo-mechanical processes between 600 to 800°C temperature range, as a result cracks are also observed in AEH-4 (Table 4.2). The porosity in air entrained HSC is, therefore, beneficial in reducing cracking at elevated temperatures by allowing thermal expansion of aggregates, absorbing the stress due to internal thermo-chemical changes and vapor movement. The observed cracks (marked in white) in Fig. 4.13 clearly illustrate that in AEH, the damage to paste aggregate interface, as well as mortar cracking, is minimum, as a result, the usual problem of high temperature aggregate-paste thermal incompatibility is reduced. The minimum amount of cracks in air entrained high strength concrete, therefore, substantiates enhanced fire resistance in AEH mixes.

4.2.3 Scanning electron microscopy:

Since, the properties of concrete are highly dependent on its microstructure so the use of scanning electron microscopy technique is helpful for in depth study of concrete regarding its characterization and evaluation of certain parameters affecting strength of concrete (Stutzman 2001). With increase in temperature there is a decay in microstructure of concrete is observed which decrease its mechanical strength properties (Demirel and Keleştemur 2010; Peng and Huang 2008). As in this study it can be seen that air entrained mixtures are exhibiting lesser loss in mechanical strength which is attributed to the presence of air entrained concrete. In order to figure out the role of air particles in details the microstructure of air entrained concrete mixtures was

studied with scanning electron microscopy technique (ASTMC1723-10 2014). AEH-4 mixtures was selected in order to study the role of entrained air voids at microstructural level.

It can be seen from the Fig. 4.4 below that at room temperature microstructure of concrete is comprising on C-S-H gel, $Ca(OH)_2$ and ettringite which is the typical microstructure of concrete (Diamond 1972). No cracks can be seen at this temperature. However, at temperature ranges from 100°C to 200°C (Fig. 4.5 & 4.6) some cracks can be observed in microstructure running through the matrix. These cracks are supposed to be in $Ca(OH)_2$ crystals and in un hydrated cement particles (Lin et al. 1996). Moreover, it is clear that no decomposition of any type of microstructural entities has taken place at this temperature range, because at this temperature range only water evaporates also no considerable change in air voids can be seen at this temperature.
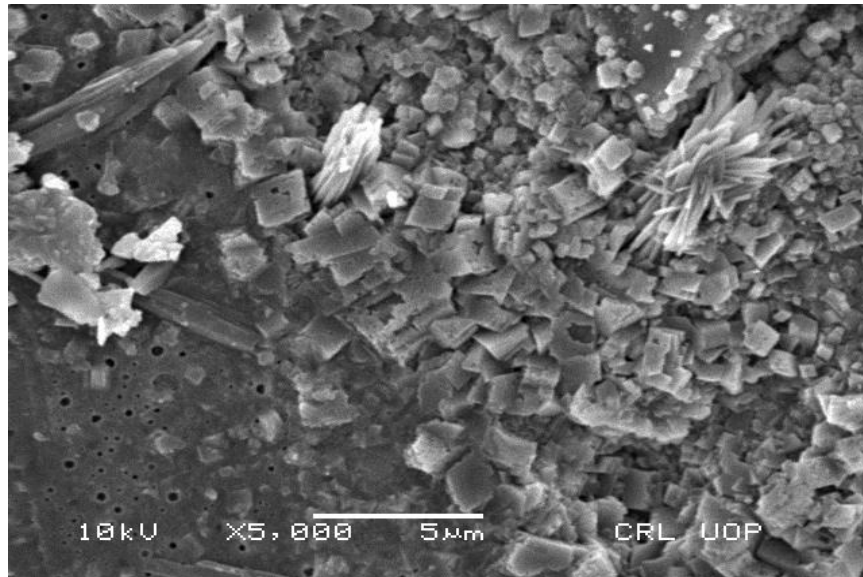
Fig. 4.4 Scanning Electron Microscope image at 23°C
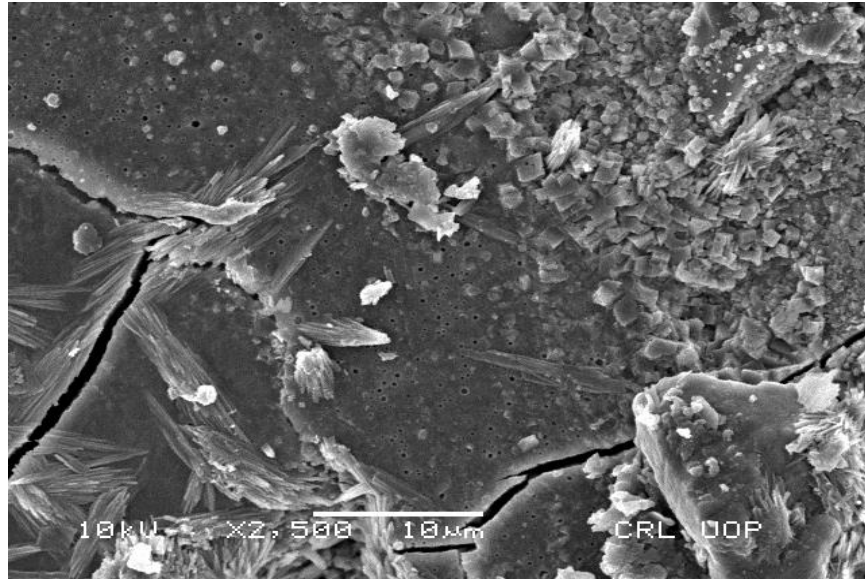
Fig. 4.5 Scanning Electron Microscope image at 100°C
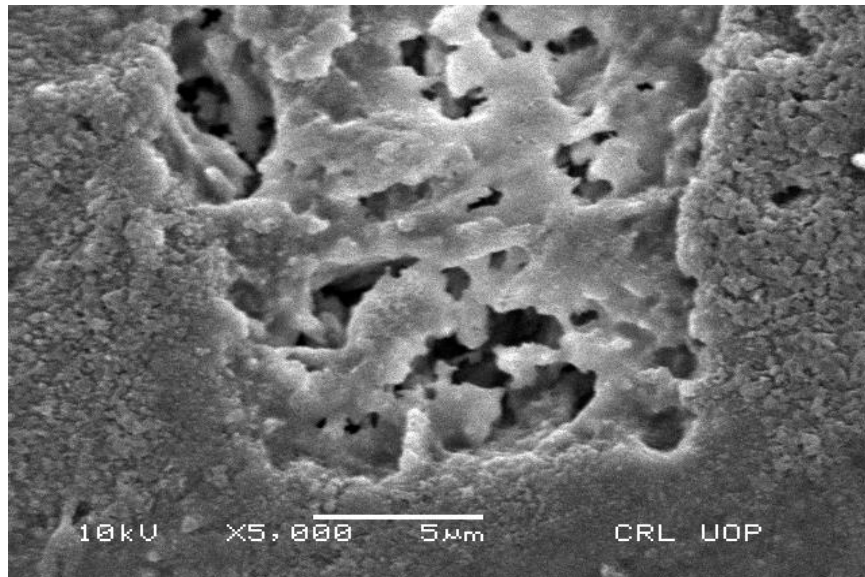
Fig. 4.6 Scanning Electron Microscope image at 200°C

At the temperature value of 400°C to 600°C (Fig. 4.7 & 4.8), it can be clearly seen that air voids

appearing in the previous images are no more present at this temperature range. It can be attributed

to the fact that aggregate content (especially coarse) of concrete expands at high temperature values

and space created by air voids acts as cushion and provides room for aggregate expansion. Hence,

the air voids are filled up at elevated temperatures and are not visible further
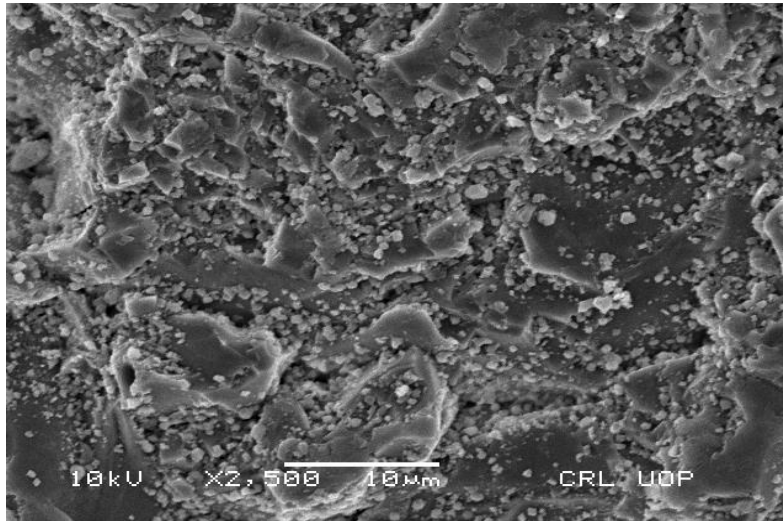
Fig. 4.7 Scanning Electron Microscope image at 400°C

At the temperature value of 800°C (Fig. 4.9), it can be seen that the microstructure of C-S-H gel

has been changed considerably, which can be attributed to its decomposition. Moreover, it can be

seen that there are gaps/voids in the microstructure which are may be due to the fact that at 800°C,

the C-S-H gel shrinks and calcium based aggregate decomposes above 600°C creating voids in

microstructure.
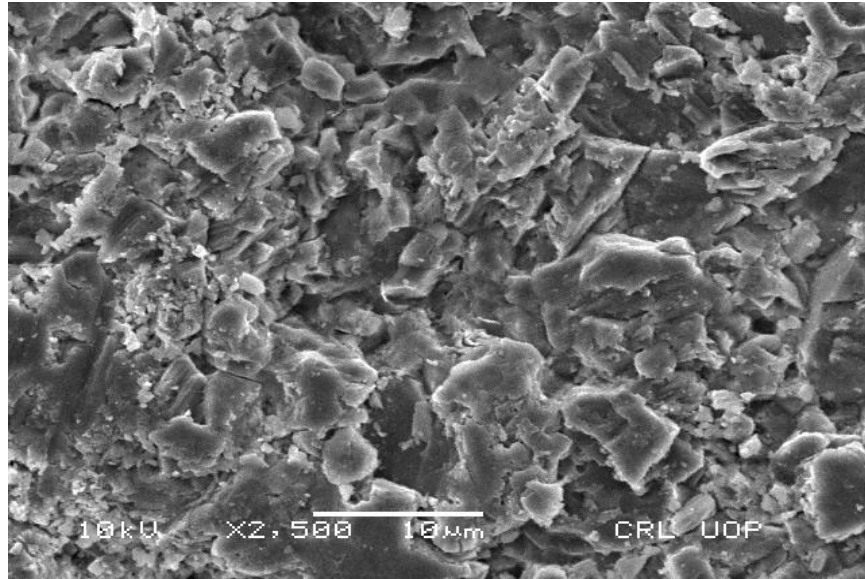
Fig. 4.8 Scanning Electron Microscope image at 600°C
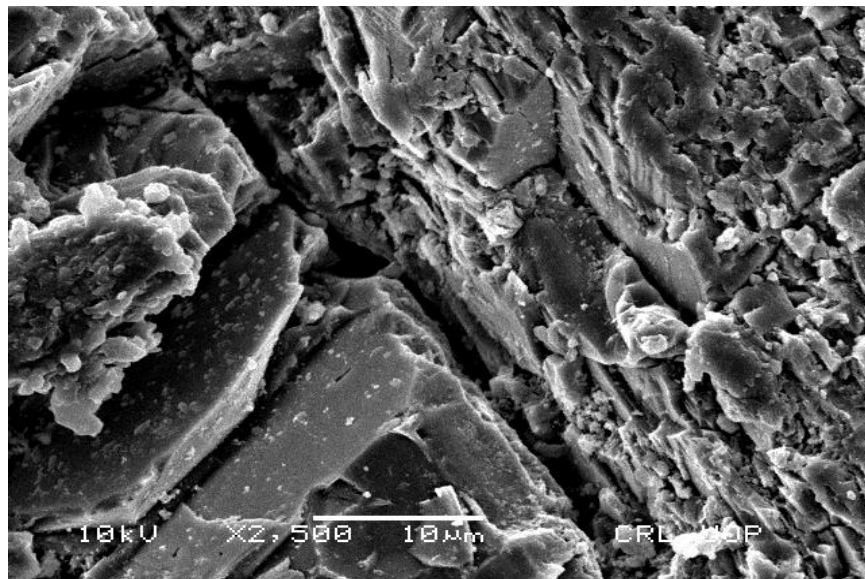
Fig. 4.9 Scanning Electron Microscope image at 800°C

4.3 Mechanical properties

Mechanical properties of all the series mixtures are discussed here

4.3.1 Compressive strength

The results of compressive strength tests at elevated temperature for unstressed ($f'_{c,T}$) and residual test ($f'_{c,T(res)}$) conditions are presented here.

4.3.1.1 Residual test conditions results

For residual test conditions the maximum drop with increase in temperature was observed for NAEH-1 mixture which was 80% at 100 and 200°C, and 50% at 400°C respectively. At temperature above 400°C, the specimen spalled off due to heating hence no compressive strength tests were carried out beyond 400°C for NAEH-1 mixture. After NAEH-1 mixture, the highest strength loss with increase in temperature was observed in NAEH-2 mixture specimen which was 83, 83 52, and 26% for 100, 200, 400, and 600°C respectively. Likewise NAEH-1, NAEH-2 mixture specimens were spalled off beyond 600°C hence no compressive strength test was carried out after 600°C for NAEH-1 mixture. After that highest compressive strength loss was measured in AEH-8 mixture specimen which was 81%, 82%, 62%, 31%, and 14% at 100°C, 200°C, 400°C, 600°C, and 800°C respectively. For AEH-4 mixture specimen the compressive strength loss was 89, 90, 65, 35, and 16% at 100, 200, 400, 600, and 800°C respectively.

4.3.1.2 Unstressed test conditions results

For unstressed test conditions, the order of compressive strength loss in mixtures was similar as for residual test conditions. For NAEH-1 mixture the compressive strength loss was 67% for 100°C, 67.5% for 200°C, and 53% for 400°C. For NAEH-2 mixture specimen it was 69%, 69.5%, 55%, and 37% for 100, 200, 400 and 600°C respectively. For AEH-8 mixture specimen, it was 70%, 70.7%, 65%, 43%, and 20% for 100, 200, 400, 600 and 800°C respectively. For AEH-4

mixture specimen the compressive strength loss was 72%, 72.3%, 67%, 45% and 22% for 100, 200, 400, 600 and 800°C respectively.
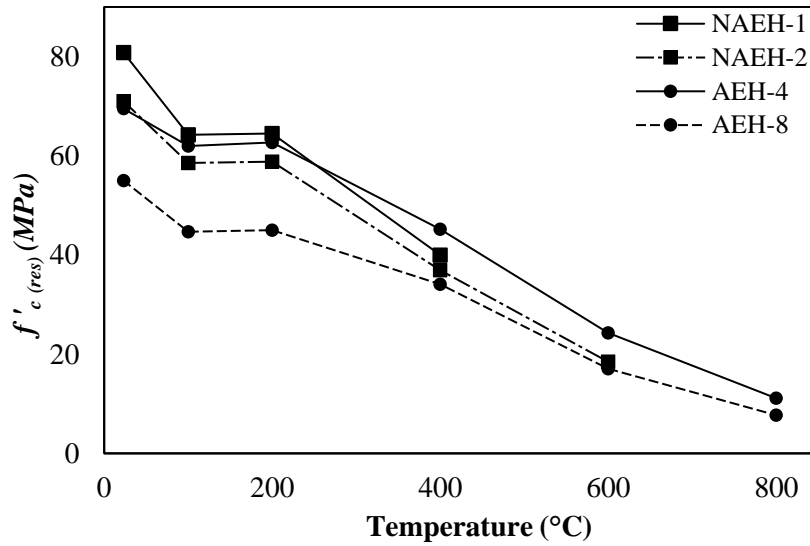
Fig. 4.10 Plot showing drop in absolute compressive strength with increase in temperature in residual test conditions
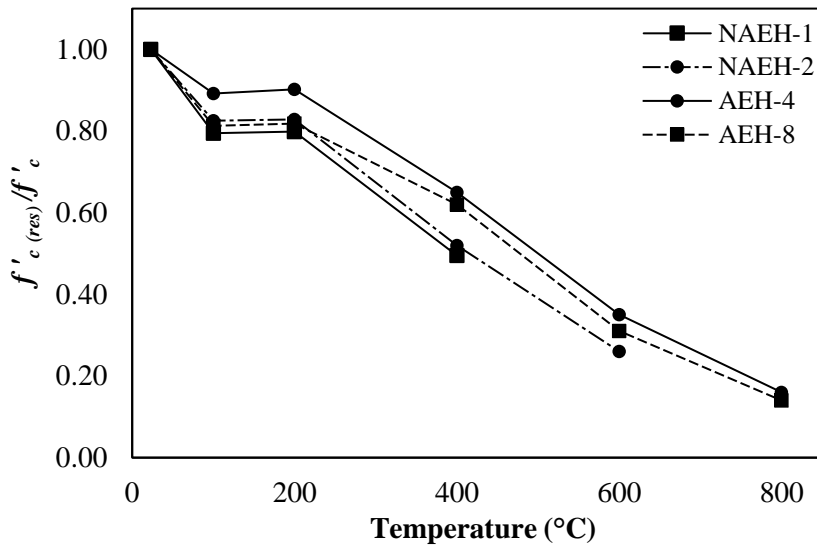
Fig. 4.10 Plot showing relative drop in compressive strength with increase in temperature in residual test conditions
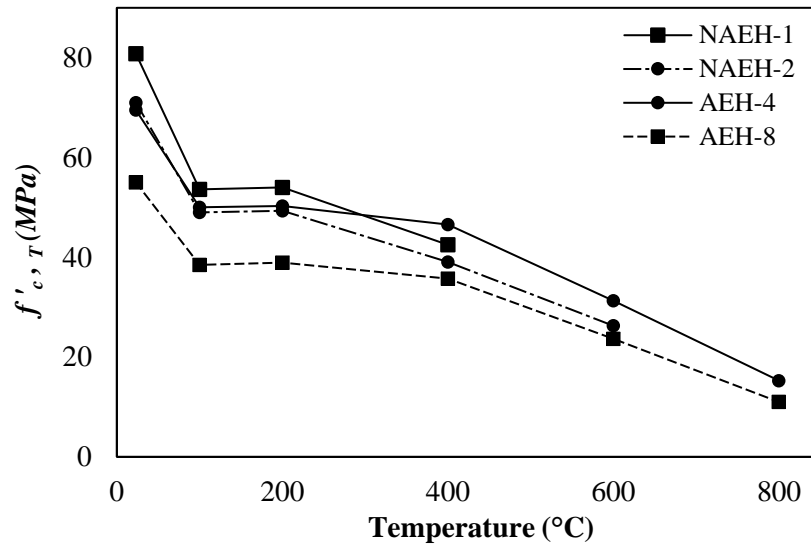
Fig. 4.11 Plot showing absolute drop in compressive strength with increase in temperature in unstressed test conditions
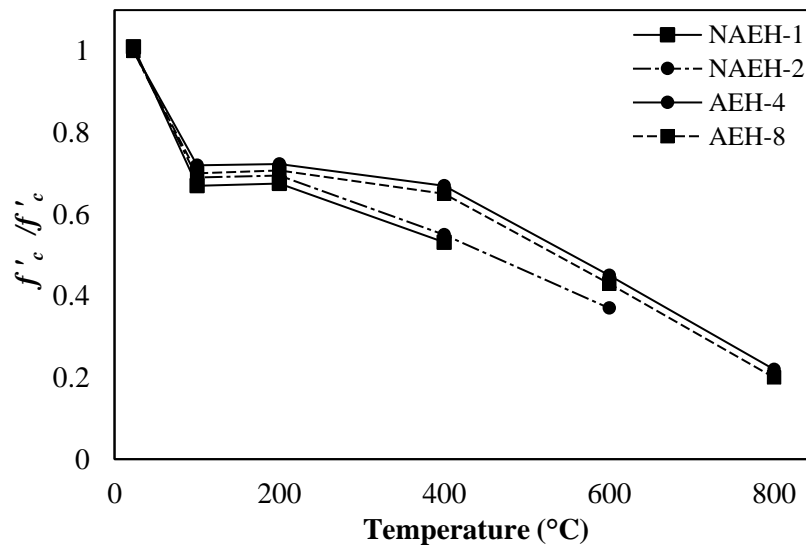
Fig. 4.12 Plot showing relative drop in compressive strength with increase in temperature in unstressed test conditions

It shows Fig. 4.10 to Fig. 4.12 that at 100°C, the loss of free and adsorbed water initiates (Bažant and Kaplan 1996; Khoury 1992) and results in major loss of strength between 10% to 33% in all four concrete types. This initial loss at 100°C is quite higher (between 31% and 33%) both air and non-air entrained concretes. This is attributed to the disturbances in van der walls forces on loss of

moisture initially attenuating the bonding forces in calcium silicate hydrate (C-S-H) gel due to dehydration. Between 100 to 200°C, strength loss is negligible which is attributed to the increase in surface forces between C-S-H gel resulting from loss of adsorbed water in paste which is a typical phenomenon that is observed in most types of concrete (Castillo 1987; Castillo and Durrani 1990; Hoff et al. 2000; Phan and Carino 2002). As the evaporation of adsorbed water depends upon the microstructural density in concrete, it usually evaporates at around 200°C in NSC owing to lower microstructure density, similarly to that observed in AEH concretes.

The temperature higher than 400°C causes disintegration of C-S-H gel, as C-S-H gel shrinks due to evaporation of moisture as well as expansion of aggregates occur at this temperature (Behnood and Ghandehari 2009; Georgali and Tsakiridis 2005; Hoff et al. 2000). This simultaneous shrinkage and expansion cause deterioration in aggregate-paste bond. As a result, large strength degradation is observed in all four types of concrete mixes. The loss in strength between 400 to 600°C is attributed to decomposition of calcium hydroxide. This can be attributed to decomposition of calcium hydroxide ($Ca(OH)_2$) that occurs mainly between 400 to 600°C (Bažant and Kaplan 1996; Behnood and Ghandehari 2009; Castillo and Durrani 1990) and decarbonation of calcium carbonate ($CaCO_3$) which mostly occurs between 600 to 800°C temperatures range (Bažant and Kaplan 1996; Castillo and Durrani 1990; Khoury 1992; Lankard et al. 1971; Lie and Kodur 1996). A further drop in compressive strength between 600 to 800°C was observed due to calcination of limestone aggregates as limestone based coarse aggregates were used in mix for this study.

It is observed from the test data (Fig. 4.10 to Fig. 4.12) that, comparatively air entrained high strength concrete exhibits lesser loss in compressive strength throughout 23 to 800°C temperature

range. Air entrainment helps reduce stresses in microstructure that result from loss of free and adsorbed water giving easy passage to evaporating water due to large air passages available uniformly throughout the matrix. The loss in strength in AEH specimens is low as expansion of aggregates and shrinkage of calcium silicate gel are relatively prevented in air entrained specimens as the usage of air entraining agent reduces the shrinkage phenomenon in mortars (Kronlöf et al. 1995). Moreover, homogenously introduced and uniformly distributed air acts as cushion for thermal expansion of aggregates. The point of space availability for thermal expansion of aggregates can be observed from Fig. 4.13 which shows two AEH-4 specimens at 23°C and that exposed to 800°C respectively. It is evident that almost all the space which was due to entrainment of air is covered by aggregates at higher temperature. The reduced shrinkage phenomenon in air entrained concrete prevents the weakening of bond between aggregate and gel. Moreover, availability of space for expansion of aggregates also prevents deterioration of C-S-H gel being compressed. This leads to reduced loss in compressive strength in air entrained concrete in comparison to non-air entrained concrete.

A comparison of strength loss in air entrained concrete specimens AEH-4 and AEH-8 in Fig. 4.10 to Fig. 4.12 shows that a higher air content draws a higher loss in strength with rising temperatures. For each mix regime, there exists a quantity of air percentage which exactly carries all the vapors produced at a specified temperature and provides space to the gel and aggregates. Further increase in air percentage from that threshold value is not believed beneficial. Based on this study, out of two air entraining percentages used, 4% air content can be considered as a threshold value for optimum strength.

a) AEH-4 specimen cross
section at 23°C

b) AEH-4 Specimen cross
section at 800°C
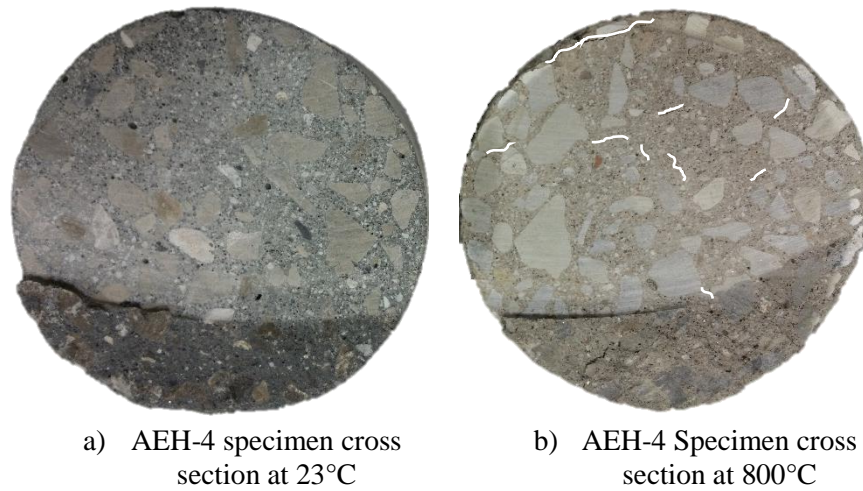
Fig. 4.13 Comparison of cross section of Air entrained specimen at 23°C and 800°C

4.3.2 Splitting tensile strength

The results of compressive strength tests at elevated temperature for unstressed ($f'_{t,T}$) and residual test ($f'_{t,T\,(res)}$) conditions are presented here.

4.3.2.1 Residual test condition results

Fig. 4.14 Drop in splitting tensile strength with increase in temperature for residual test conditions

Fig. 4.15 Relative Drop in splitting tensile strength with increase in temperature for residual test conditions

4.3.2.2 Unstressed test condition results

For residual test conditions highest loss in split tensile strength among all the mixes was observed for NAEH-1. The 28 days split tensile strength for this mix at 23°C was 5.7 MPa and at 400°C this strength value was 2.56 MPa which is 45% of strength at 23°C. After NAEH-1 the highest loss in strength was observed in NAEH-2 mixture. The tensile strength at 23°C was 5.1 MPa and at 600°C this value was dropped to 1.53 MPa which is just 30% of strength at 23°C. The behavior of air entrained mixture specimen was again well than non-air entrained concrete. The loss in strength of both air entrained mixes was almost same. The 23°C tensile strength was 5.1 and 4.6 MPa for AEH-4 and AEH-8 respectively, and this value was dropped to 0.87 MPa and 0.74 MPa which is 17% and 16% of room temperature strength, respectively.

Like compressive strength loss, the order of loss in split tensile strength in unstressed test conditions among mixes was similar with the order of loss in split tensile strength of residual test conditions. For NAEH-1 the split tensile strength at 400°C was 2.7 MPa which is 47% of room

temperature strength. For NAEH-1 the split tensile strength at 600°C was 1.6 MPa which is 31% of room temperature strength. For AEH-4 and AEH-8 the split tensile strength at 800°C was 1.2 MPa and 1 MPa which is 24% and 22% of room temperature strength.
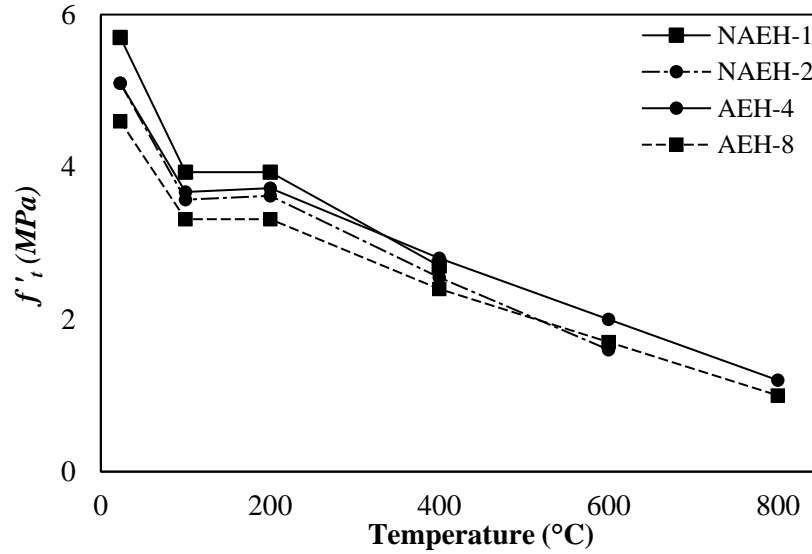
Fig. 4.16 Drop in splitting tensile strength with increase in temperature for unstressed test conditions
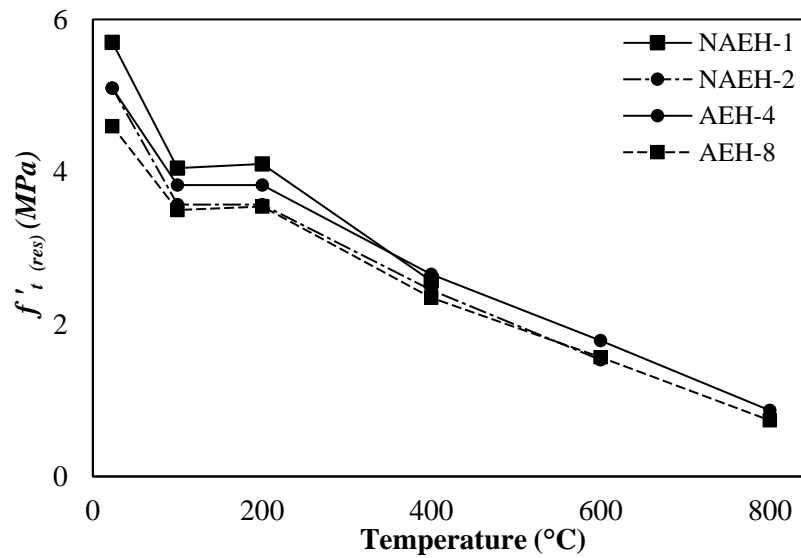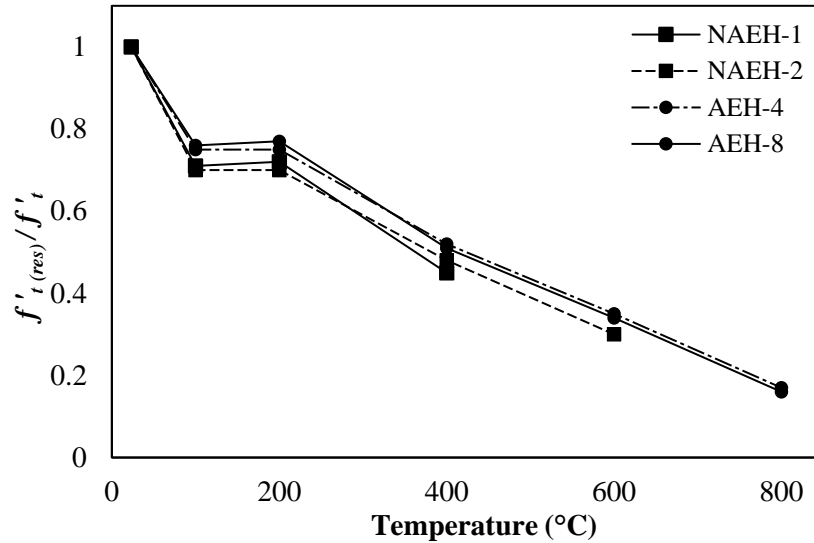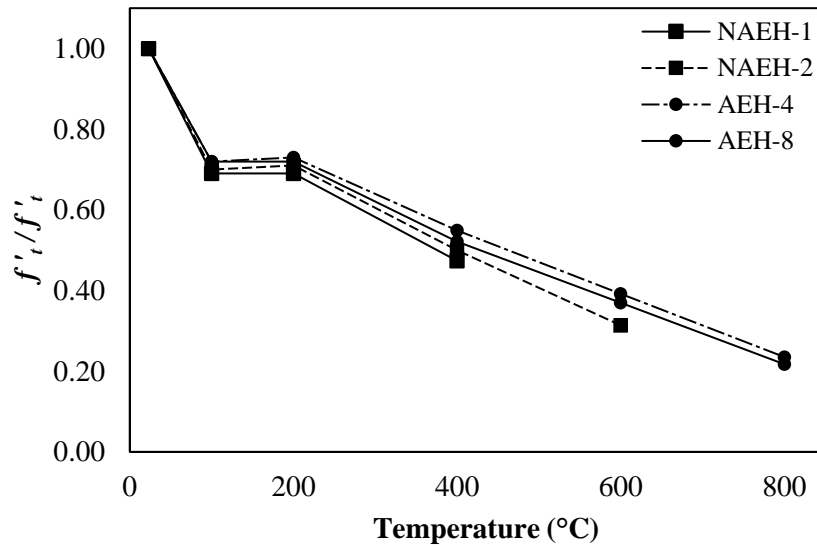

Fig. 4.17 Relative drop in splitting tensile strength with increase in temperature for unstressed test conditions

83

For unstressed (hot) and residual test conditions, the tensile strength behavior of air entrained concrete specimens is better than that of non-air entrained concrete specimens. The microstructural changes explained for loss in compressive strength are also responsible for tensile strength drop with increase in temperature for non-air entrained concrete. Moreover, the reduced shrinkage due to usage of air entraining agents at high temperatures and availability of space for expansion of coarse aggregates are primary cause of improved tensile strength behavior of air entrained concrete.

It can be ascertained from Figs. 4.10 to 4.12 and Figs. 4.15 to 4.17 that loss in tensile strength with increase in temperature is higher than the loss in compressive strength which is in agreement with previous studies (Behnood and Ghandehari 2009; Khaliq and Kodur 2011). This rapid loss in tensile strength is attributed to the microcracks development due to the thermal incompatibility of aggregates and C-S-H gel (Chan et al. 1999; Khoury 1992). Tensile strength is more sensitive to this thermal incompatibility than compressive strength. Moreover, it is also observed that improvement in tensile behavior of concrete, due to porosity introduced in it by polypropylene fibers, is lower than the improvement in compressive behavior. It is similar to the findings observed in literature that air entrainment effects compressive strength more than splitting tensile strength (Behnood and Ghandehari 2009). Comparison between air entrained AEH-4 and AEH-8 mixes shows that splitting tensile strength loss follows same trend and therefore no direct relationship is observed between increased air percentage. This conforms to the observation that increased porosity and lesser loss in tensile strength has no relation as in the case of using polypropylene fibers (Behnood and Ghandehari 2009).

4.3.3 Stress-Strain Response

To capture the stress strain response of specimen in compression displacement of specimen is recorded with the help of linear variable displacement transducer (LVDTs) attached on specimen and corresponding load values are recorded with the load controlled compression testing machine. The loading rate was according to ASTM C39/C39M-16b (2016) but loading machine was load controlled. An effort was made to capture post peak response with load controlled method using extremely controlled loading rate. Like other mechanical tests, stress strain plot was captured for both unstressed and residual test conditions. Stress strain plot results are shown in such a way that a comprehensive comparison can be made among mixtures stress strain plots. NAEH-1 and AEH-4 mixture stress strain plots, NAEH-2 and AEH-4 mixture stress strain plots and AEH-4 and AEH-8 mixture stress strain plots are plotted side by side on same scale. All results for residual and unstressed test conditions are shown first, after that results are discussed and explained.

4.3.3.1 Residual stress strain response

4.3.3.1.1 NAEH-1 and AEH-4
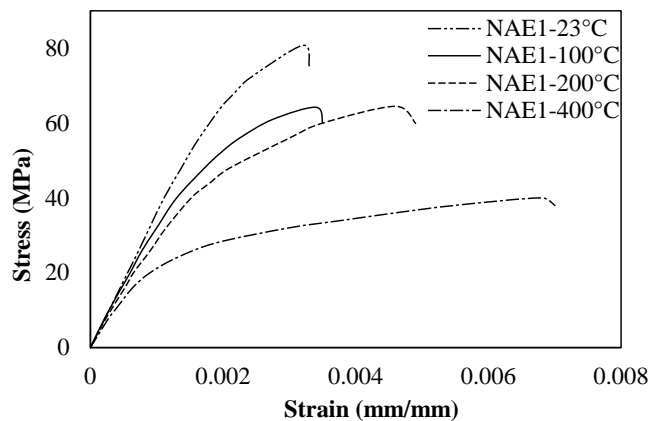
a)   Stress strain plot of NAEH-1 mixture from 23°C to 400°C   b)   Stress strain plot of AEH-4 mixture from 23°C to 800°C
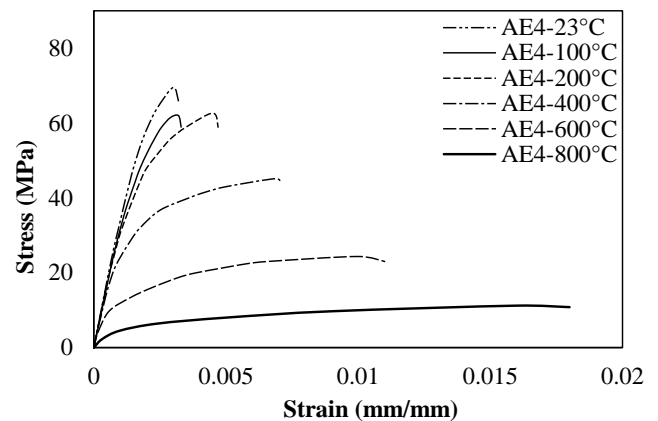
Fig. 4.18 Residual Stress strain plot of NAEH-1 mixture specimen and AEH-4 mixture specimen

4.3.3.1.2 NAEH-2 and AEH-4
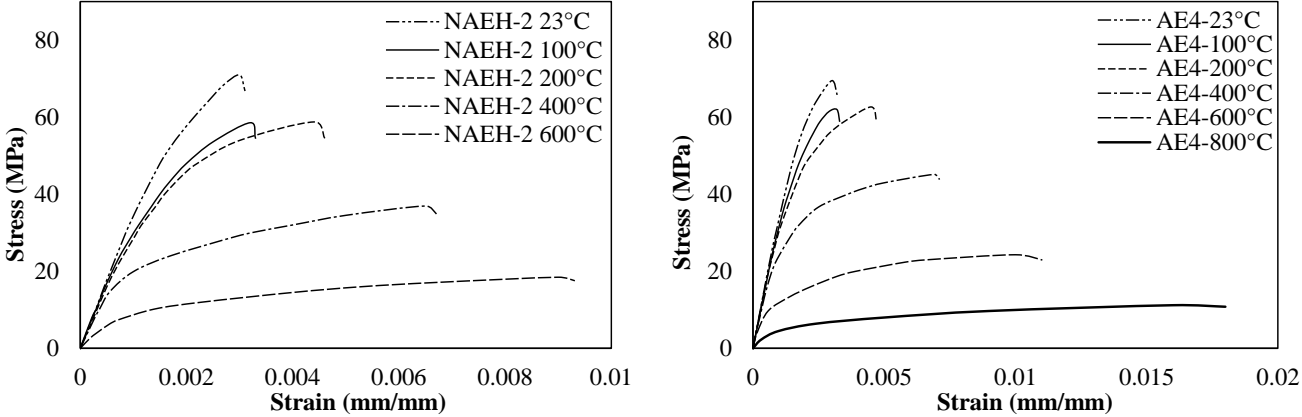
a)   Stress strain plot of NAEH-2 mixture from 23°C to 600°C

b)   Stress strain plot of AEH-4 mixture from 23°C to 800°C

Fig. 4.19 Residual Stress-Strain plot of NAEH-2 mixture specimen and AEH-4 mixture specimen

4.3.3.1.3 AEH-4 and AEH-8
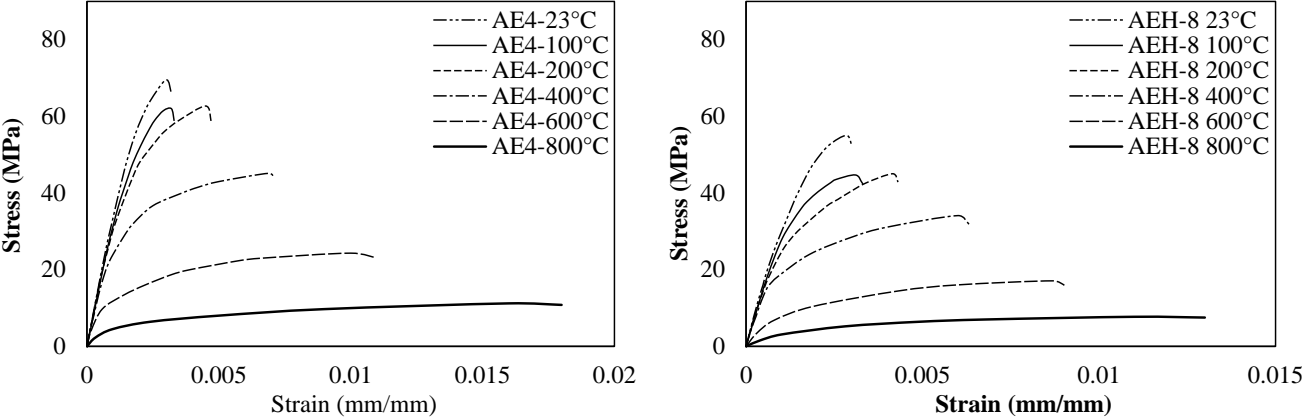
a)   Stress strain plot of AEH-4 mixture from 23°C to 800°C

b)   Stress strain plot of AEH-8 mixture from 23°C to 800°C

Fig. 4.20 Residual Stress-Strain plot of AEH-4 mixture specimen and AEH-8 mixture specimen

4.3.3.2 Unstressed stress strain response

4.3.3.2.1 NAEH-1 and AEH-4
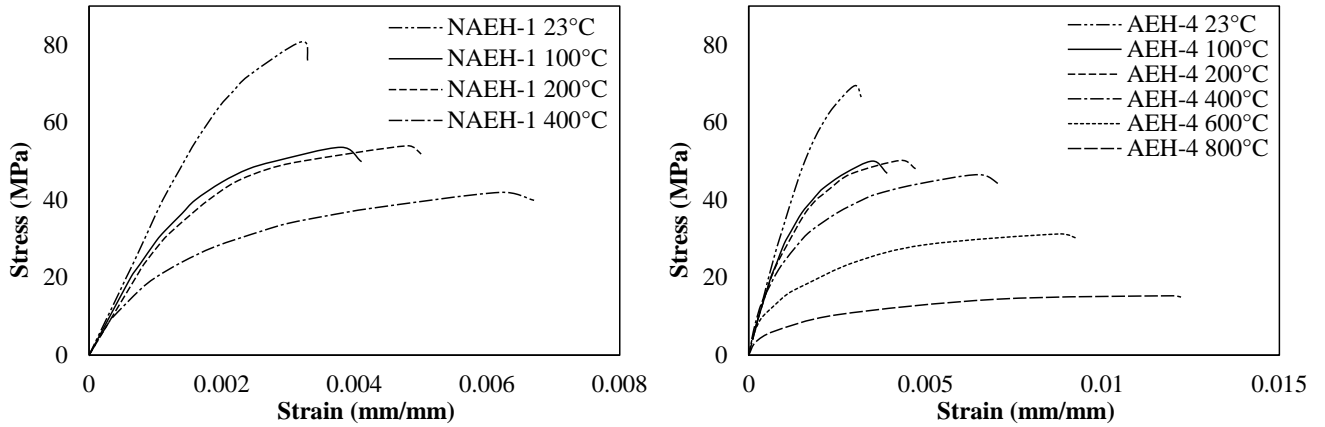
a)   Stress strain plot of NAEH-1 from 23°C to 400°C

b)   Stress strain plot of AEH-4 from 23°C to 800°C

Fig. 4.21 Unstressed Stress strain plot of NAEH-1 mixture specimen and AEH-4 mixture specimen

4.3.3.2.2 NAEH-2 and AEH-4
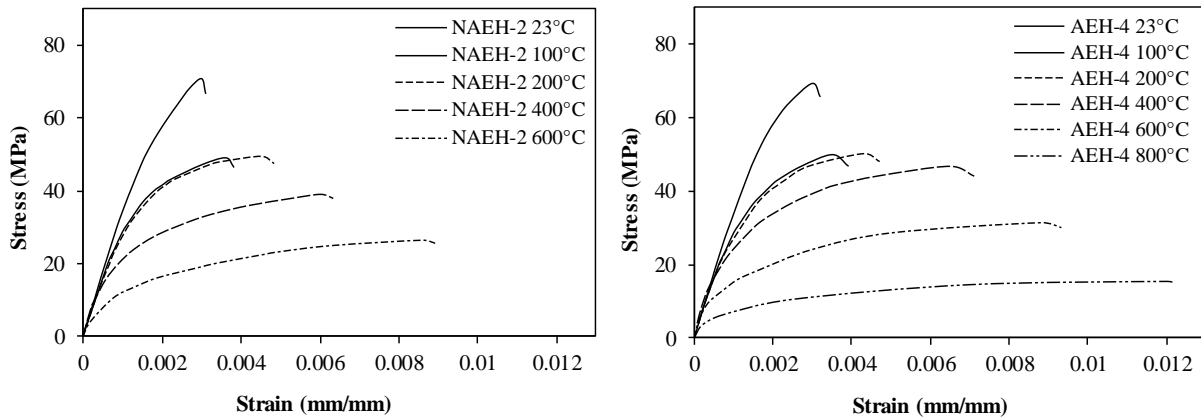
a)   Stress strain plot of NAEH-2 from 23°C to 600°C

b)   Stress strain plot of AEH-4 from 23°C to 800°C

Fig. 4.22 Unstressed stress strain plot of NAEH-2 mixture specimen and AEH-4 mixture specimen

4.3.3.2.3 AEH-4 and AEH-8
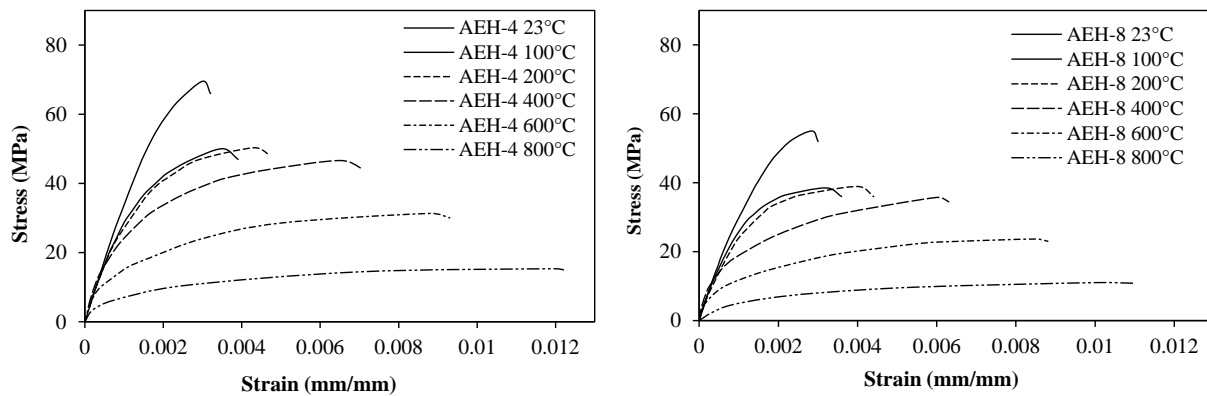
a)   Stress strain plot of AEH-4 from 23°C to 800°C

b)   Stress strain plot of AEH-8 from 23°C to 800°C

Fig. 4.23 Unstressed stress strain plot of AEH-4 mixture specimen and AEH-8 mixture specimen

A common trend in stress-strain response of tested HSC types in Figs. 4.18 to 4.23 shows that the strains at peak stresses increase for all the mixes with increase in temperature. In almost all cases, there is an initial decrease in peak stress and corresponding increase in strain from room to 200°C, however, further increase in temperature results in much lower stresses and higher corresponding strains at 400, 600 and 800°C temperatures. This behavior is typical for concrete at elevated temperatures which is attributed to moisture loss, macro and microstructural deteriorations involving mortar cracking, bond disintegration due to paste-aggregate thermal incompatibility, decomposition of $Ca(OH)_2$, decarbonation of $CaCO_3$, disintegration of C-S-H gel, and thermal creep at higher temperatures (Castillo and Durrani 1990; Cheng et al. 2004; Khaliq and Khan 2015). Although this behavior is shown by both air and non-air entrained HSC, however, stress-strain data in Figs. 4.19 and 4.22 exhibits that AEH-4 concrete shows relatively higher strain values compared to NAEH-2 concrete at each target temperature. This is attributed to easy movement of moisture owing to space availability, resulting in higher ductility in AEH at all temperatures. This

fact is further strengthened as can be seen from Figs. 4.20 and 4.23 that with increase in air content from AEH-4 to AEH-8, much higher strain values are obtained with decrease in corresponding stresses at all temperature ranges in AEH-8 concrete.

Limited captured post-peak behavior in Figs. 4.18 and 4.23 shows that the post peak stress-strain response becomes flatter with the increase in temperature and decrease in corresponding stresses. This is attributed to the intrinsic property of concrete that concrete having lesser strength possess flatter post peak response as shown in the several stress-strain models of concrete (Popovics 1970). The results, therefore, conform to prior studies for stress-strain response changing from brittle to ductile with increase in temperature (Castillo and Durrani 1990). Overall, the increase in peak strain values for air-entrained mixes are higher than non-air entrained ones which depict a much ductile behavior of air entrained mixes. Moreover, higher the air content higher are the strain values but with much less corresponding stress values with increase in temperatures.

4.3.4   Elastic modulus:

Static modulus of elasticity according to ASTM C469/C469M-14 (2014) was calculated from above shown stress strain plots for both unstressed and residual test conditions.

Compressive stress-strain curves at elevated temperatures were used to calculate elastic modulus for NAEH and AEH concretes as per ASTM C469/C469M-14 (2014) test standards. Elastic modulus was calculated at strains corresponding to 40% of stress values at each target temperature for all mix specimens and the variation in elastic modulus is shown in Figs. 4.24 to 4.27. The figures show that the effect of elevated temperatures on loss of elastic modulus is roughly same for both air and non-air entrained concrete types. Overall, the variability in rate of loss of elastic modulus is considerable at 100°C, steadies up to 400°C, however rate in loss is quite higher at

temperatures between 400 to 800°C and minimal at 800°C. The initial loss of modulus up to 100°C

is attributed to loss of free and capillary moisture from concrete microstructure. After initial

disturbances due to moisture phase changes, physical deterioration reduces between 100 to 400°C

temperature range, as a result, loss in elastic modulus steadies. However, above 400°C all the

thermochemical and thermomechanical disturbances follow namely, aggregate-paste bond

deterioration due to thermal incompatibilities, onset of decomposition of C-S-H and $Ca(OH)_2$ at

about 450°C, calcination of $CaCO_3$ that occurs at 550°C onwards, and high temperature creep that

sets in above 650°C (Bažant and Kaplan 1996; Castillo and Durrani 1990). Therefore, all these

factors are attributing to higher rate of loss in elastic modulus between 400 to 800°C temperature

range as shown in Fig. 8 for both NAEH and AEH concretes.

4.3.4.1 Residual conditions test results
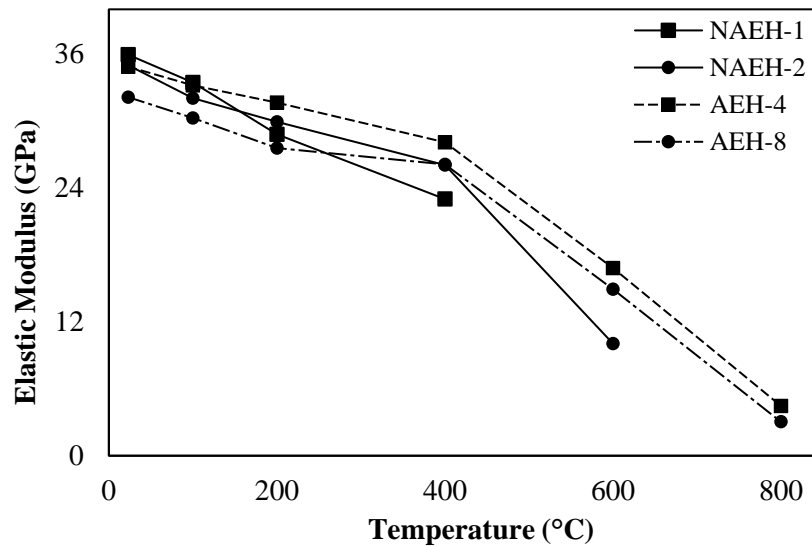
Fig. 4.24 Plot showing absolute drop in elastic modulus with increase in temperature for residual test conditions
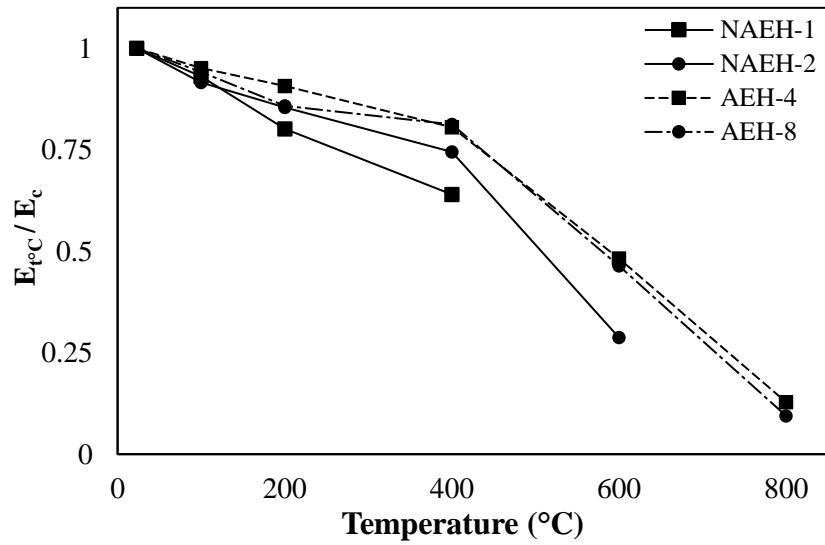
Fig. 4.25 Plot showing drop in relative elastic modulus with increase in temperature for residual test conditions

4.3.4.2 Unstressed conditions test results
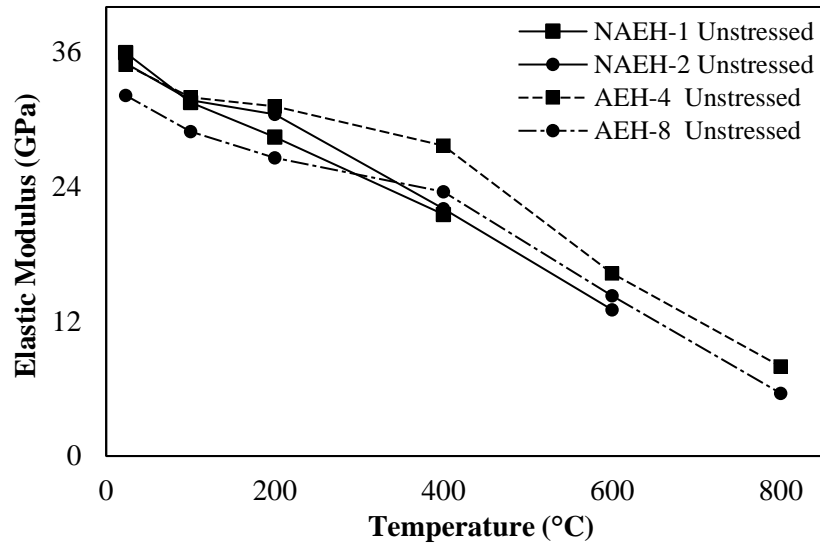
Fig. 4.26 Plot showing absolute drop in elastic modulus with increase in temperature for unstressed conditions
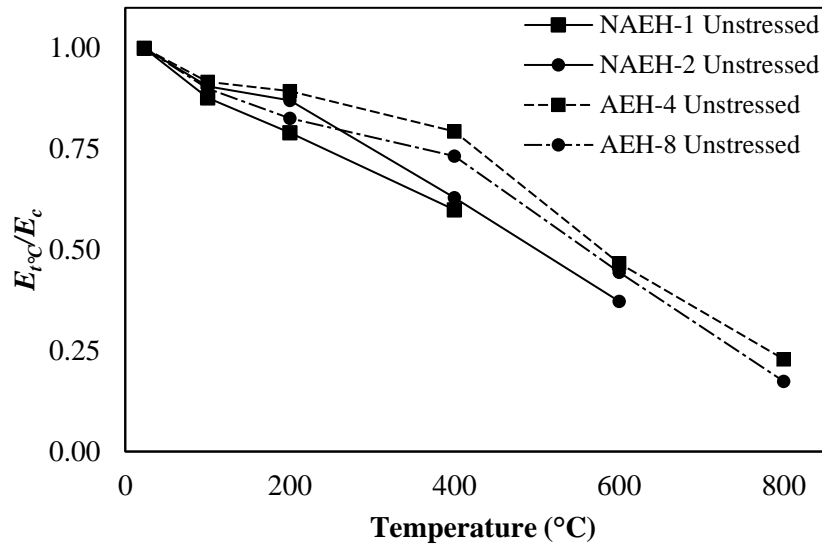
Fig. 4.27 Plot showing relative drop in elastic modulus with increase in temperature for unstressed conditions

Figs. 4.24 and 4.26 show absolute and Figs. 4.25 and 4.27 show normalized variation in elastic modulus as a function of temperature for all four concrete types and for both unstressed and residual test conditions. It is evident that the trends in loss of elastic modulus are similar, however, the relative loss is lower in case of air entrained concrete especially in the important temperature range of 400 to 800°C. Compared to NAEH, it is observed that with increase in air content, initial values of elastic modulus are lower in AEH, however, retention of modulus is better than NAEH throughout the temperature range. The elastic modulus is not lost much in all types of mixes up to 400°C temperature, as on the average about 73% to 83% modulus is retained in NAEH and AEH respectively. Further, when the NAEH could not sustain temperatures beyond 600°C due to fire induced spalling, AEH concretes retained 25% and 18% of elastic modulus at 800°C for AEH-4 and AEH-8 concretes respectively. It also confirms that HSC exhibiting higher loss in compressive strength will also exhibit more loss in elastic modulus (Castillo 1987; Phan et al. 2001). The drop in elastic modulus of air entrained mixes (AEH-4 and AEH-8) is lesser than non-air entrained mixes (NAEH-1 and NAEH-2) as shown in Figs. 4.24 to 4.27. It was expected because these mixes

were experiencing lesser loss in compressive strength. The relative drop in AEH-4 and AEH-8 mixes is almost similar with a marginal difference which is again due to the saturation effect of porosity. The improved behavior in AEH is also attributed to distributed porosity resulting from air entrainment, similarly to improved elastic modulus in HSC due to porosity resulting from melting of polypropylene fibers at elevated temperatures (Khaliq and Kodur 2011).

4.3.5   Mass loss

Mass loss is linked to loss of moisture present in various forms in concrete namely free, capillary, absorbed, adsorbed, and chemically combined water. As the temperature increases the loss of moisture takes place at various rates depending upon the heating conditions, hydro-thermal processes, bonding conditions of water, and microstructure density of concrete. Mass loss results at various temperatures are represented as ratio of mass as target temperature to that at room temperature (M_T/M) as shown in Figs 4.28 and 4.29. It can be observed from figure that mass loss occurs at different rates with increase in temperature in all four types of concrete specimens tested, however, it is evident as expected that higher mass loss is observed in air entrained concrete specimens. It can also be seen that predominantly, rate of mass loss is lower from room to 100°C temperature, increases between 100 to 200°C, steadies till 600°C and again increases with higher rate between 600 to 800°C.

All four concrete types had lower mass loss up to 100°C can be attributed to the fact that phase change of moisture from liquid to vapor takes place up to 100°C, moreover initially moisture is a cause of stress on capillary network as it makes its way to escape from the concrete microstructure by disturbing the meniscus equilibrium within capillaries. This is the reason that there is higher loss of both compressive and splitting tensile strength up to 100°C in both air and non-air entrained

concrete types (Figs. 4.10 to 4.12 and Figs. 4.15 to 4.17). Highest rate of mass loss is observed between 100 and 200°C in air entrained concrete in both test conditions. This is attributed to phase change of water above 100°C involving higher activity of hydro-thermal processes and opening up and coalescence of microstructural passages along with higher permeability of air entrained concrete, which allows easy movement for vapor.

With initial loss of free moisture, the mass loss turns steady between 200 and 600°C temperature range. This is the temperature range when along with adsorbed water, chemically combined water starts loosening but at a lower rate. Owing to mineral admixtures used in for air entrained HSC, higher amount of C-S-H gel is available in the system having well-combined moisture in this nano-sized hydrated compound. As a result, comparatively lower rate of moisture loss is observed. A higher rate of mass loss is again observed in 600 to 800°C temperature range in air entrained concrete specimens. This is attributed to dissociation of calcium carbonate that occurs between 600 and 650°C and results in liberation of dissociated CO_2 (Lie and Kodur 1996). It also results in deterioration of microstructure of concrete including cracks and fissures (Fig. 4.13b) resulting in higher permeation that allows releasing the inward migrated and entrapped vapor clog as well as chemically combined water.

Mass loss difference between NAEH-1 and NAEH-2 mixes is not significant and variation in rate of mass loss is only between 3% to 10% up to 600°C for these specimens as shown in Figs 4.28 and 4.29. In the case of AEH-4 and AEH-8 specimens, rate of mass loss was higher which varied from 10% at 200°C to 22% at 800°C. Overall, highest mass loss was observed in AEH-8 specimens which is attributed to large air space and void system allowing moisture to escape easily in higher

quantity. Conversely, lowest mass loss was observed in NAEH-1 specimens which is attributed to dense microstructure not allowing easy escape of water vapor (Mindeguia et al. 2010).
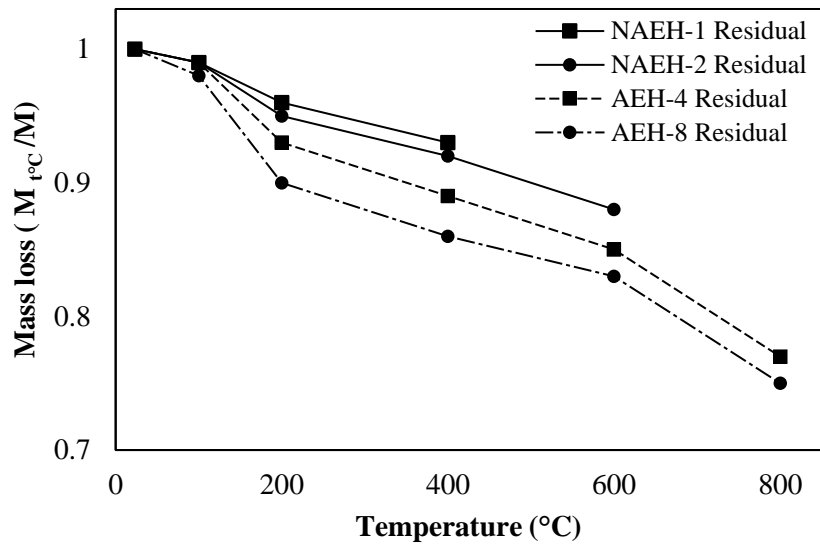
Fig. 4.28 Relative drop in mass with increase in temperature for residual test conditions
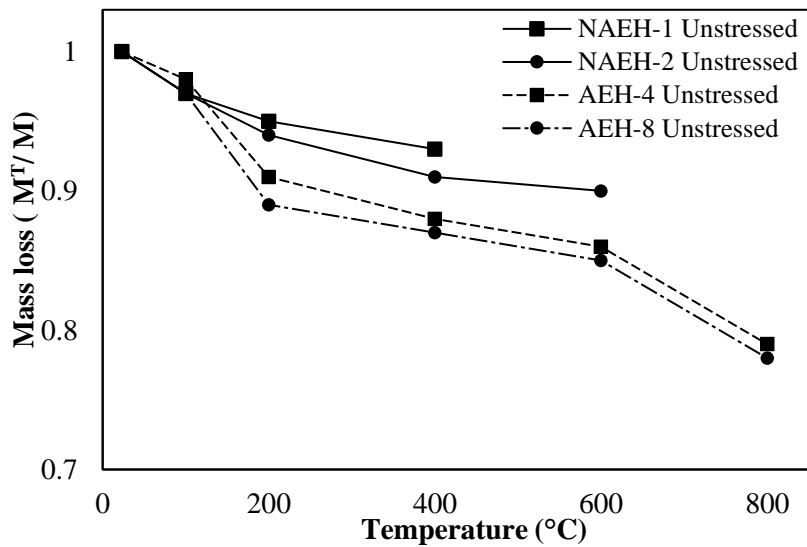
Fig. 4.29 Relative drop in mass with increase in temperature for unstressed test conditions

3.3 Mathematical Relations

To ascertain the fire behavior of RC structural members, full scale testing is required under controlled fire scenarios which are time, effort and financially demanding. Alternately, analytical

models help predict fire behavior of structures using known mechanical properties with relative ease. Data obtained in present test regime was used to develop simplified mathematical relationships for high temperature mechanical properties of AEH. In this study, linear regression analysis utilizing method of least squares is applied (Wackerly et al. 2008) and simple equations are obtained with the help of commercial software (Minitab 2017). The temperature was taken as independent variable and loss in relevant strength was treated as dependent variable. The accuracy of the mathematical relations can be predicted with the coefficient of determination R^2. The value of R^2 closer to 100% means describes accuracy of the model or vice versa. In this study, the mathematical models of air entrained high strength concrete mixes (AEH-4) are provided, whereas mathematical models for conventional high strength concrete are available elsewhere (Khaliq 2012).

The variation of compressive strength ($f'_{c,T}$), tensile strength ($f'_{t,T}$), elastic modulus (E_T), and mass loss (M_T) with temperature is related through coefficients α_T and β_T representing ratio of respective strength at target temperature ($f'_{c,T}, f'_{t,T}, E_T,$ and M_T) to that at room temperature (f'_c, f'_t, E, and M) for AEH-4 and AEH-8 concrete respectively for both residual and unstressed test conditions. In lieu of equations, reduction factors α_T and β_T, at different temperatures can be used for evaluating compressive and tensile strength, elastic modulus, and mass loss for AEH-4 concrete. These reduction factors are also shown here. Both equations and reduction factors for AEH-4 and AEH-8 can be incorporated in analytical studies for fire performance predictions of structural members made of air entrained HSC.

4.3.6.1 Mathematical relationships for residual test conditions

Mathematical models for AEH-4 mixture for compression, splitting tensile strength, elastic modulus and mass loss for residual test conditions are shown below

Table 4.3 High Temperature property relationship for AEH-4 concrete

Property	Mathematical Relationship
Compressive strength	$\alpha_{T,compression} = 1.0507 - 0.0011 \, x \, T \quad 23°C \leq T \leq 800°C$
Splitting tensile strength	$\alpha_{T,tensile} = 0.9371 - 0.001 \, x \, T \quad 23°C \leq T \leq 800°C$
Elastic modulus	$\alpha_{T,modulus} = 1.0969 - 0.0011 \, x \, T \quad 23°C \leq T \leq 800°C$
Mass loss	$\alpha_{T,mass} = 1.0062 - 0.0003 \, x \, T \quad 23°C \leq T \leq 800°C$

The reduction factors as mentioned above for AEH-4 mixture are tabulated below

Table 4.4 High temperature properties reduction factors for AEH-4 concrete

(°C)	Reduction factor α_T for AEH-4			
	Compressive strength	Tensile strength	Elastic modulus	Mass loss
23	1	1	1	1
100	0.94	0.84	0.99	0.98
200	0.83	0.74	0.88	0.95
400	0.61	0.54	0.66	0.89
600	0.39	0.34	0.44	0.83
800	0.17	0.14	0.22	0.77

Similarly, mathematical relationships for AEH-8 mixture for residual test conditions are shown below

Table 4.5 High Temperature property relationship for AEH-8 concrete

Property	Mathematical relationships
Compressive strength	$\beta_{T,compression} = 0.9985 - 0.0011 \, x \, T \quad 23°C \leq T \leq 800°C$
Splitting tensile strength	$\beta_{T,\,tensile} = 0.9471 - 0.001 \, x \, T \quad 23°C \leq T \leq 800°C$
Elastic modulus	$\beta_{T,\,modulus} = 1.0866 - 0.0011 \, x \, T \quad 23°C \leq T \leq 800°C$
Mass loss	$\beta_{T,\,mass} = 0.994 - 0.0003 \, x \, T \quad 23°C \leq T \leq 800°C$

Reduction factors based on above mentioned relationships for AEH-8 mixture is tabulated below

Table 4.6 High temperature properties reduction factors for AEH-8 concrete

(°C)	Reduction factor β_T for AEH-8			
	Compressive strength	Tensile strength	Elastic modulus	Mass loss
23	1	1	1	1
100	0.89	0.85	0.98	0.96
200	0.78	0.75	0.87	0.93
400	0.56	0.55	0.65	0.87
600	0.34	0.35	0.43	0.81
800	0.12	0.15	0.21	0.75

4.3.6.2 Mathematical relationships for unstressed test conditions

Mathematical relations for AEH-8 mixture regarding drop in mechanical strength and for unstressed conditions are shown below

Table 4.7 High temperature property relationship for AEH-4 concrete

Property	Mathematical relationship
Compressive strength	$\alpha_{T,compression} = 0.99 - 0.0008T \quad 23°C \leq T < 200°C$
Splitting tensile strength	$\alpha_{T,tensile} = 0.9118 - 0.0009T \quad 23°C \leq T \leq 800°C$
Elastic modulus	$\alpha_{T,modulus} = 1.0609 - 0.001T \quad 23°C \leq T \leq 800°C$
Mass loss	$\alpha_{T,mass} = 0.992 - 0.0002T \quad 23°C \leq T < 800°C$

Reduction factors for AEH-8 mixture for unstressed test conditions based on above relationships are tabulated below

Table 4.8 High temperature properties reduction factors for AEH-4 concrete

Temperature (°C)	Reduction factor α_T for AEH-4			
	Compressive strength	Tensile strength	Elastic Modulus	Mass Loss
23	1	1	1	1
100	0.85	0.82	0.96	0.97
200	0.77	0.73	0.86	0.95
400	0.61	0.55	0.66	0.91
600	0.45	0.37	0.46	0.87
800	0.29	0.19	0.26	0.83

Similarly, mathematical relationships for AEH-8 mixture regarding drop in mechanical strength with increase in temperature for unstressed test conditions are tabulated below

Table 4.9 High temperature property relationship for AEH-8 concrete

Property	Mathematical relationships
Compressive strength	$\beta_{T,\,compression} = 0.9167 - 0.0009 \; x \; T \quad 23°C \leq T < 200°C$
Splitting tensile strength	$\beta_{T,\,tensile} = 0.909 - 0.0009 \; x \; T \quad\;\; 23°C \leq T \leq 800°C$
Elastic modulus	$\beta_{T,\,modulus} = 1.0381 - 0.001 \; x \; T \quad\; 23°C \leq T \leq 800°C$
Mass loss	$\beta_{T,\,mass} = 0.9831 - 0.0003 \; x \; T \quad 23°C \leq T < 800°C$

Reduction factors for AEH-8 mixture for unstressed test conditions based on above equations are tabulated below

Table 4.9 High temperature properties reduction factors for AEH-8 concrete

Temperature (°C)	Reduction factor β_T for AEH-8			
	Compressive strength	Tensile strength	Elastic Modulus	Mass Loss
23	1	1	1	1
100	0.83	0.82	0.94	0.95
200	0.74	0.73	0.84	0.92
400	0.56	0.55	0.64	0.86
600	0.38	0.37	0.44	0.80
800	0.20	0.19	0.24	0.74

<div align="right">**CHAPTER 5**</div>

CONCLUSIONS AND RECOMMENDATIONS

5.1   General

This study discusses the mechanical properties of HSC and compares it with AEHSC at elevated temperatures including 23, 100, 200, 400, 600, 800°C under residual and unstressed test conditions. In addition to mechanical properties, spalling behavior is also studied and discussed in this study along with the cracks analysis and color change of specimen with increase in temperature. This chapter covers the conclusions which are drawn after analyzing the results from experiments performed in this research program. After that future recommendations on further research on this topic are discussed.

5.2   Conclusions

Following conclusions can be drawn based on above results

- Spalling is observed in both non-air entrained HSC mixture specimens i.e. NAEH-1 and NAEH-2 at furnace air chamber temperature of above 400 and 600°C, respectively. In contrast to that, no spalling is observed in both air entrained HSC mixture specimens i.e. AEH4 and AEH8.

- The cracking pattern on concrete specimen was observed for all four mix regimes with increase in temperature. However, cracking analysis was done for two mix regimes i.e. NAEH-2 and AEH4. For NAEH-2 mixture regime specimens, the cracking initiated between temperature range of 200 to 400°C, however the cracking pattern is not dense. A denser cracking pattern is observed at 600°C which becomes denser at 800°C. For AHE4 mix regime specimen, there

can be seen no cracking pattern at temperatures up to 400°C. A very less dense cracking pattern is observed at 600°C which becomes denser at 800°C.

- The loss in relative compressive strength for air entrained HSC is lesser as compared to non-air entrained HSC at all temperature values. However, the difference is not significant up to 200°C. At the temperature values above 200°C, the difference in relative compressive strength decrement becomes significant.

- The loss in relative tensile strength of concrete specimen at elevated temperature for air and non-air entrained HSC follows same trend as observed in relative loss in compressive strength. The relative loss in tensile strength in air entrained HSC mixture specimen is less as compared to air entrained HSC and difference becomes significant at temperature above 200°C.

- Despite of loss in peak stress, increase in temperature causes increase in strain corresponding to peak stress for all four mixtures. The difference in strain at room temperature and strain at any elevated temperature among four mixtures is very slight.

- Like drop in compressive strength, drop in elastic modulus is also observed for all four mixtures. For temperature value of 200°C, the difference in elastic modulus is not significant and drop in elastic modulus is slightly greater for non-air entrained mixtures. The difference becomes significant at temperature values more than 200°C and drop in elastic modulus is greatest for NAEH-1.

- Increase in temperature causes the drop in specimen mass for all the mixtures. This drop in mass becomes significant above temperature value of 100°C. The lowest mass drop is observed in mixture with most dense microstructure i.e. NAEH-1 and highest mass drop is observed in mixture containing highest entrained air i.e. AEH-4.

5.3   Recommendations

- The role of entrained air in high strength concrete mixtures under fire is elaborated in this study through detailed testing program. However, there are some future research recommendation which are necessary in order to carry out in-depth study on this subject. Such recommendation are listed in the following:

- Several air void systems with different chord lengths and specific surfaces can be introduced in high strength concrete mixtures and their fire performance can be evaluated with detailed tests and their results can be compared. In this way, the performance of entrained air in high strength concrete under fire can be optimized.

- Poly-propylene fibers can also be incorporated in concrete mixture along with entrained air and their performance can be studied collectively.

- Columns, beams or slabs can be cast with reinforced concrete having entrained air in it and full scale testing can be performed on various standard fire curves.

- Different types of SRMs can also be incorporated in mixture regimes along with air entrainment in concrete and their effect can be studied.

REFERENCES

ACI 211.4-08 (2008). "211.4 R-08: Guide for Selecting Proportions for High-Strength Concrete Using Portland Cement and Other Cementitious Materials."

ACI (2013). "CT-13 ACI Concrete Terminology." 2013.

ACI, C.-. "State of the Art Report on High-Strength Concrete." *Proc., ACI Journal Proceedings*, ACI.

Aıtcin, P. (2003). "The durability characteristics of high performance concrete: a review." *Cement and Concrete Composites*, 25(4), 409-420.

Anderberg, Y. "Spalling phenomena of HPC and OC." *Proc., NIST Workshop on Fire Performance of High Strength Concrete in Gaithersburg*, 69-73.

ASTM C39/C39M-16b (2016). "Standard test method for compressive strength of cylindrical concrete specimens." ASTM International, West Conshohocken, PA. www.astm.org.

ASTM C192/C192M-16a (2016). "Standard practice for making and curing concrete test specimens in the laboratory." ASTM International, West Conshohocken, PA. www.astm.org.

ASTM C457/C457M-12 (2012). "Standard test method for microscopical determination of parameters of the air-void system in hardened concrete." ASTM International, West Conshohocken, PA. www.astm.org.

ASTM C469/C469M-14 (2014). "Standard test method for static modulus of elasticity and Poisson's ratio of concrete in compression." ASTM International, West Conshohocken, PA. www.astm.org.

ASTM C617/C617M-15 (2015). "Standard practice for capping cylindrical concrete specimens." ASTM International, West Conshohocken, PA. www.astm.org.

ASTMC33/C33M-13 (2013). "Standard Specification for Concrete Aggregates." ASTM International West Conshohocken, PA.

ASTMC78/C78M-10 (2010). "Standard Test Method for Flexural Strength of Concrete (Using Simple Beam with Third-Point Loading." ASTM International West Conshohocken, PA.

ASTMC260/C260M-10a (2010). "Standard Specification for Air-Entraining Admixtures for Concrete." ASTM International West Conshohocken, PA.

ASTMC494/C494M-15 (2015). "Standard Specification for Chemical Admixtures for Concrete." ASTM International West Conshohocken, PA.

ASTMC496-11 (2011). "Standard Test Method for Splitting Tensile Strength of Cylindrical Concrete Specimens." ASTM International West Conshohocken, PA.

ASTMC618-08a (2008). "Standard Specification for Coal Fly Ash and Raw or Calcined Natural Pozzolan for Use in Concrete." ASTM International West Conshohocken, PA.

ASTMC1231/C1231M-12 (2012). "C1231/C1231M-12."." *Practice for Use of Unbonded Caps in Determination of Compressive Strength of Hardened Concrete Cylinders." ASTM International*.

ASTMC1240-15 (2015). "Standard Specification for Silica Fume Used in Cementitious Mixtures." ASTM International West Conshohocken, PA.

ASTMC1583/1583M-13 (2013). "Standard Test Method for Tensile Strength of Concrete Surfaces and the Bond Strength or Tensile Strength of Concrete Repair and Overlay Materials by Direct Tension (Pull-off Method)." ASTM International West Conshohocken, PA.

ASTMC1723-10 (2014). "Standard Guide for Examination of Hardened Concrete Using Scanning Electron Microscopy." ASTM International West Conshohocken, PA.

ASTME1868-10 (2015). "Standard Test Methods for Loss-On-Drying by Thermogravimetry." ASTM International West Conshohocken, PA.

Baalbaki, M., and Aitcin, P. (1994). "Cement/superplasticizer/air-entraining agent compatibility." *ACI Special Publication*, 148.

Bastami, M., Chaboki-Khiabani, A., Baghbadrani, M., and Kordi, M. (2011). "Performance of high strength concretes at elevated temperatures." *Scientia Iranica*, 18(5), 1028-1036.

Bazant, Z. P. "Analysis of pore pressure, thermal stress and fracture in rapidly heated concrete." *Proc., International workshop on fire performance of high-strength concrete*, 155-164.

Bažant, Z. P., and Kaplan, M. F. (1996). *Concrete at high temperatures: material properties and mathematical models*, Longman Group Limited, Essex, England.

Behnood, A., and Ghandehari, M. (2009). "Comparison of compressive and splitting tensile strength of high-strength concrete with and without polypropylene fibers heated to high temperatures." *Fire Safety Journal*, 44(8), 1015-1022.

Behnood, A., and Ziari, H. (2008). "Effects of silica fume addition and water to cement ratio on the properties of high-strength concrete after exposure to high temperatures." *Cement and Concrete Composites*, 30(2), 106-112.

Benjamin, I. (1962). "Fire resistance of reinforced concrete." *Special Publication, ACI SP 5-02*, 5, 25-39.

Bouguerra, A., Ledhem, A., De Barquin, F., Dheilly, R., and Queneudec, M. (1998). "Effect of microstructure on the mechanical and thermal properties of lightweight concrete prepared from clay, cement, and wood aggregates." *Cement and concrete research*, 28(8), 1179-1190.

Carino, N. (1994). "Effects of testing variables on the strength of high-strength (90 MPa) concrete cylinders." *Special Publication SP 149-34, ACI*, 149, 589-632.

Castillo, C. (1987). "Effect of transient high temperature on high-strength concrete." Rice University.

Castillo, C., and Durrani, A. J. (1990). "Effect of transient high temperature on high strength concrete." *ACI Materials Journal*, 87(1), 47-53.

Chan, S. Y. N., Peng, G.-F., and Anson, M. (1999). "Fire behavior of high-performance concrete made with silica fume at various moisture contents." *ACI Materials Journal*, 96(3), 405-409.

Chan, Y., Luo, X., and Sun, W. (2000). "Compressive strength and pore structure of high-performance concrete after exposure to high temperature up to 800°C." *Cement and Concrete Research*, 30(2), 247-251.

Chan, Y., Peng, G., and Anson, M. (1999). "Residual strength and pore structure of high-strength concrete and normal strength concrete after exposure to high temperatures." *Cement and Concrete Composites*, 21(1), 23-27.

Chen, B., and Liu, J. (2004). "Residual strength of hybrid-fiber-reinforced high-strength concrete after exposure to high temperatures." *Cement and Concrete Research*, 34(6), 1065-1069.

Cheng, F.-P., Kodur, V., and Wang, T.-C. (2004). "Stress-strain curves for high strength concrete at elevated temperatures." *Journal of Materials in Civil Engineering*, 16(1), 84-90.

Chia, K.-S., and Zhang, M.-H. (2007). "Workability of air-entrained lightweight concrete from rheology perspective." *Magazine of Concrete Research*, 59(5), 367-375.

Committee, A. (2011). "Building Code Requirements for Structural Concrete (ACI 318-11) and Commentary." *Farmington Hills*.

Demirel, B., and Keleştemur, O. (2010). "Effect of elevated temperature on the mechanical properties of concrete produced with finely ground pumice and silica fume." *Fire Safety Journal*, 45(6), 385-391.

Diamond, S. (1972). "Identification of hydrated cement constituents using a scanning electron microscope energy dispersive X-ray spectrometer combination." *Cement and Concrete Research*, 2(5), 617-632.

Freeman, E., Gao, Y.-M., Hurt, R., and Suuberg, E. (1997). "Interactions of carbon-containing fly ash with commercial air-entraining admixtures for concrete." *Fuel*, 76(8), 761-765.

Fu, Y., and Li, L. (2011). "Study on mechanism of thermal spalling in concrete exposed to elevated temperatures." *Materials and structures*, 44(1), 361-376.

Gebler, S., and Klieger, P. (1983). "Effect of fly ash on the air-void stability of concrete." *ACI Special Publication*, 79.

Georgali, B., and Tsakiridis, P. (2005). "Microstructure of fire-damaged concrete. A case study." *Cement and Concrete Composites*, 27(2), 255-259.

Giergiczny, Z., Glinicki, M. A., Sokołowski, M., and Zielinski, M. (2009). "Air void system and frost-salt scaling of concrete containing slag-blended cement." *Construction and Building Materials*, 23(6), 2451-2456.

Han, C.-G., Hwang, Y.-S., Yang, S.-H., and Gowripalan, N. (2005). "Performance of spalling resistance of high performance concrete with polypropylene fiber contents and lateral confinement." *Cement and concrete research*, 35(9), 1747-1753.

Harada, T., Takeda, J., and S Yamane, F. F. (1972). "Strength, elasticity and thermal properties of concrete subjected to elevated temperatures." *ACI Special Publication*, 34.

Hertz, K. D. (2005). "Concrete strength for fire safety design." *Magazine of Concrete Research*, 57(8), 445-453.

Hoff, G. C., Bilodeau, A., and Malhotra, V. M. (2000). "Elevated temperature effects on HSC residual strength." *Concrete International*, 22(4), 41-48.

Husem, M. (2006). "The effects of high temperature on compressive and flexural strengths of ordinary and high-performance concrete." *Fire Safety Journal*, 41(2), 155-163.

Jackson, F. H. (1944). "Concretes Containing Air-Entraining Agents." *JOURNAL OF THE AMERICAN CONCRETE INSTITUTE*.

Jackson, F. H., and Timms, A. G. (1954). "Evaluation of Air-Entraining Admixtures for Concrete." *Public Roads*.

Janotka, I., and Nürnbergerová, T. (2005). "Effect of temperature on structural quality of the cement paste and high-strength concrete with silica fume." *Nuclear Engineering and design*, 235(17), 2019-2032.

Kakizaki, M., Edahiro, H., Tochigi, T., and Niki, T. (1992). "Effect of mixing method on mechanical properties and pore structure of ultra high-strength concrete." *ACI Special Publication*, 132.

Kalifa, P., Menneteau, F.-D., and Quenard, D. (2000). "Spalling and pore pressure in HPC at high temperatures." *Cement and concrete research*, 30(12), 1915-1927.

Khaliq, W. (2012). "Performance characterization of high performance concretes under fire conditions [Ph. D. thesis]." Michigan State University.

Khaliq, W., and Khan, H. A. (2015). "High temperature material properties of calcium aluminate cement concrete." *Construction and Building Materials*, 94, 475-487.

Khaliq, W., and Kodur, V. (2011). "Effect of high temperature on tensile strength of different types of high-strength concrete." *ACI Materials Journal*, 108(4).

Khaliq, W., and Kodur, V. (2011). "Thermal and mechanical properties of fiber reinforced high performance self-consolidating concrete at elevated temperatures." *Cement and Concrete Research*, 41(11), 1112-1122.

Khaliq, W., and Kodur, V. (2012). "High temperature mechanical properties of high-strength fly ash concrete with and without fibers." *ACI Materials Journal*, 109(6).

Khoury, G. (1992). "Compressive strength of concrete at high temperatures: a reassessment." *Magazine of concrete Research*, 44(161), 291-309.

Kim, H., Jeon, J., and Lee, H. (2012). "Workability, and mechanical, acoustic and thermal properties of lightweight aggregate concrete with a high volume of entrained air." *Construction and Building Materials*, 29, 193-200.

Kodur, V. "Spalling in high strength concrete exposed to fire — concerns, causes, critical parameters and cures." *Proc., Proceedings, ASCE Structures Congress, Philadelphia, PA*, 1-8.

Kodur, V., Cheng, F.-P., Wang, T.-C., and Sultan, M. (2003). "Effect of strength and fiber reinforcement on fire resistance of high-strength concrete columns." *Journal of Structural Engineering*, 129(2), 253-259.

Kodur, V., and Khaliq, W. (2010). "Effect of temperature on thermal properties of different types of high-strength concrete." *Journal of materials in civil engineering*, 23(6), 793-801.

Kriesel, R., French, C. E., and Snyder, M. (1998). "Freeze-thaw durability of high-strength concrete."

Kronlöf, A., Leivo, M., and Sipari, P. (1995). "Experimental study on the basic phenomena of shrinkage and cracking of fresh mortar." *Cement and Concrete Research*, 25(8), 1747-1754.

Lamprecht, H.-O. (1993). *Opus caementitium: Bautechnik der Römer*, Beton-Verlag.

Lankard, D. R., Birkimer, D. L., Fondriest, F. F., and Snyder, M. J. (1971). "Effects of moisture content on the structural properties of portland cement concrete exposed to temperatures up to 500F." *Special Publication, ACI SP 59-102*, 25, 59-102.

Lie, T., and Kodur, V. (1996). "Thermal and mechanical properties of steel-fibre-reinforced concrete at elevated temperatures." *Canadian Journal of Civil Engineering*, 23(2), 511-517.

Lin, W.-M., Lin, T., and Powers-Couche, L. (1996). "Microstructures of fire-damaged concrete." *Materials Journal*, 93(3), 199-205.

Litvan, G. G. "Air entrainment in the presence of superplasticizers." *Proc., ACI Journal Proceedings*, ACI.

Luo, X., Sun, W., and Chan, S. Y. N. (2000). "Effect of heating and cooling regimes on residual strength and microstructure of normal strength and high-performance concrete." *Cement and Concrete Research*, 30(3), 379-383.

MacInnis, C., and Racic, D. (1986). "The effect of superplasticizers on the entrained air-void system in concrete." *Cement and Concrete Research*, 16(3), 345-352.

Menzel, C. A. (1943). *Tests of the fire resistance and thermal properties of solid concrete slabs and their significance*, National Emergency Training Center.

Mielenz, R. C., and Sprouse, J. H. (1979). "High-Range Water-Reducing Admixtures; Effect on the Air-Void System in Air-Entrained and Non-Air-Entrained Concrete." *ACI Special Publication*, 62.

Mindeguia, J.-C., Pimienta, P., Noumowé, A., and Kanema, M. (2010). "Temperature, pore pressure and mass variation of concrete subjected to high temperature — Experimental and numerical discussion on spalling risk." *Cement and Concrete Research*, 40(3), 477–487.

Mindess, S., Young, J. F., and Darwin, D. (2003). *Concrete*, Prentice Hall.

Minitab (2017). <https://www.minitab.com/>.

Peng, G.-F., and Huang, Z.-S. (2008). "Change in microstructure of hardened cement paste subjected to elevated temperatures." *Construction and Building Materials*, 22(4), 593-599.

Phan, L., Lawson, J., and Davis, F. (2001). "Effects of elevated temperature exposure on heating characteristics, spalling, and residual properties of high performance concrete." *Materials and Structures*, 34(2), 83-91.

Phan, L. T. (1996). "Fire Performance of High-Strength Concrete: A Report of the State of the Art." *National Institute of Standards and Technology, Gaithersburg, Maryland 20899*, NISTIR 5934.

Phan, L. T. "High-strength concrete at high temperature-An Overview." *Proc., Utilization of High Strength/High Perform ance Concrete, 6th International Symposium. Proceedings*, 501-518.

Phan, L. T. (2008). "Pore pressure and explosive spalling in concrete." *Materials and structures*, 41(10), 1623-1632.

Phan, L. T., and Carino, N. J. (1998). "Review of mechanical properties of HSC at elevated temperature." *Journal of Materials in Civil Engineering*, 10(1), 58-65.

Phan, L. T., and Carino, N. J. (2002). "Effects of test conditions and mixture proportions on behavior of high-strength concrete exposed to high temperatures." *ACI Materials Journal*, 99(1).

Phan, L. T., and Carino, N. J. (2003). "Code provisions for high strength concrete strength-temperature relationship at elevated temperatures." *Materials and Structures*, 36(2), 91-98.

Pigeon, M., Gagné, R., Aïtcin, P.-C., and Banthia, N. (1991). "Freezing and thawing tests of high-strength concretes." *Cement and concrete research*, 21(5), 844-852.

Pigeon, M., Plante, P., Pigeon, M., Plante, P., and Plante, M. (1989). "Air void stability, Part I: Influence of silica fume and other parameters." *ACI Materials Journal*, 86(5).

Plante, P. K., Pigeon, M., and Saucier, F. (1989). "Air-void stability, Part II: Influence of superplasticizers and cement." *ACI Materials Journal*, 86(6).

Poon, C.-S., Azhar, S., Anson, M., and Wong, Y.-L. (2003). "Performance of metakaolin concrete at elevated temperatures." *Cement and Concrete Composites*, 25(1), 83-89.

Poon, C., Shui, Z., and Lam, L. (2004). "Compressive behavior of fiber reinforced high-performance concrete subjected to elevated temperatures." *Cement and Concrete Research*, 34(12), 2215-2222.

Popovics, S. (1970). "A review of stress-strain relationships for concrete." *ACI Journal Proceedings*, 67(3), 243-248.

Powers, T. C., and Willis, T. "The air requirement of frost resistant concrete." *Proc., Highway Research Board Proceedings*.

Sanjayan, G., Stocks, L., and Stocks, L. (1993). "Spalling of high-strength silica fume concrete in fire." *ACI Materials Journal*, 90(2).

Shang, H.-S., and Yi, T.-H. (2013). "Freeze-thaw durability of air-entrained concrete." *The Scientific World Journal*, 2013.

Siebel, E. (1989). "Air-void characteristics and freezing and thawing resistance of superplasticized air-entrained concrete with high workability." *ACI Special Publication*, 119.

Stutzman, P. E. (2001). "Scanning electron microscopy in concrete petrography." *National Institute of Standards and Technology*, 2.

Wackerly, D., Mendenhall, W., and Scheaffer, R. L. (2008). *Mathematical Statistics with Applications*, Thomson Brooks/Cole.

Wright, P. J. F. "ENTRAINED AIR IN CONCRETE." *Proc., ICE Proceedings*, Thomas Telford, 337-358.

Xiao, J., and Falkner, H. (2006). "On residual strength of high-performance concrete with and without polypropylene fibres at elevated temperatures." *Fire Safety Journal*, 41(2), 115-121.

Zeiml, M., Leithner, D., Lackner, R., and Mang, H. A. (2006). "How do polypropylene fibers improve the spalling behavior of in-situ concrete?" *Cement and concrete research*, 36(5), 929-942.